Geomagnetic Secular Variation and its Changes, 1942.5 to 1962.5

S. R. C. Malin

Summary

A uniform set of geomagnetic data from observatories has been analysed
to determine secular variation of the geomagnetic field for the interval
1942.5 to 1962.5 and to reveal any changes in secular variation during
this time. The epoch to epoch changes are much smoother than have been
previously found, and permit an examination of the movements of the
centred and eccentric dipoles and changes in westward drift. The secular
variation has also been used to determine surface motions of the Earth's
core. Changes in secular variation are presented in the form of charts of
secular acceleration.

1. Introduction

Worldwide secular variation and its changes with time (secular acceleration)
are of importance because of the light they shed on processes inside the Earth and
also to reduce to a common epoch data having a spatial and temporal distribution,
for the preparation of world magnetic charts. In the present analysis models of
secular variation are deduced for the intervals 1942.5 to 1947.5, 1947.5 to 1952.5,
1952.5 to 1957.5 and 1957.5 to 1962.5. Each of the four models was derived using
the same method and the same set of data points in order to make differences between
the models as realistic as possible.

The data used in the analysis were based on annual mean values from permanent
magnetic observatories. Annual mean values are free from the effects of short
period variations and contain very little random error of observation. Although
systematic errors may still be present, providing that these do not change with time,
they do not affect secular variation which may be reliably estimated by differencing
successive annual means. It is possible that an observatory is on a local anomaly
and Cain (1967) has shown that a large local anomaly may affect the secular variation
estimate as well as the main field. However, in general, the effect is so small that
changes in the annual mean values reflect real changes in the main field.

The 11-year sunspot cycle produces an effect on the geomagnetic field, particularly
the horizontal component, which is superimposed on the longer term changes. This
phenomenon has been investigated by Yukatake (1965), who concludes that the
sunspot cycle will have a negligible effect on analyses of the rate of change of the
geomagnetic field and that most of the sunspot cycle effect is of external origin.

From a plot against time of secular variation from neighbouring observatories, it is clear that changes in secular variation are highly correlated, indicating that secular acceleration is neither a very local phenomenon nor a spurious one, such as might be caused by instrumental changes.

To interpolate worldwide values from the discrete set of points formed by observatories, spherical harmonic coefficients may be deduced. Secondary measurements of secular variation at repeat stations or from successive surveys confirm that values synthesized from the spherical harmonic coefficients in areas remote from an observatory are realistic.

2. Data

Observatory annual mean values of X, Y and Z, respectively the north, east and vertically downward components of the geomagnetic field, were taken from the list compiled at the Royal Greenwich Observatory (1967). These data are thought to be the best available since great care was taken to compare the values with those in earlier thesauri and with observatory annual volumes. Also, all the data were sent to the responsible observatories for confirmation or correction. Any apparent discontinuities in the run of values were investigated and, as far as possible, explained.

As well as means for whole years, the list contains a few means for periods of less than a year where an observatory started or finished operating other than at the end of a year, or where the records for a year were incomplete. The data for the analysis were, wherever possible, the means of five annual values centred on the required epoch (1942.5, 1947.5, 1952.5, 1957.5 and 1962.5). Where the first or last of the annual values for the five years were missing, then the means of three years, centred on the required epoch, were taken. If the first two, or last two values for the five years were missing then the mean annual value for the year of the required epoch was taken (except for Jassy, where the 1957 values stand out). If the central value was missing, then the mean of the remaining values was taken, weighted if
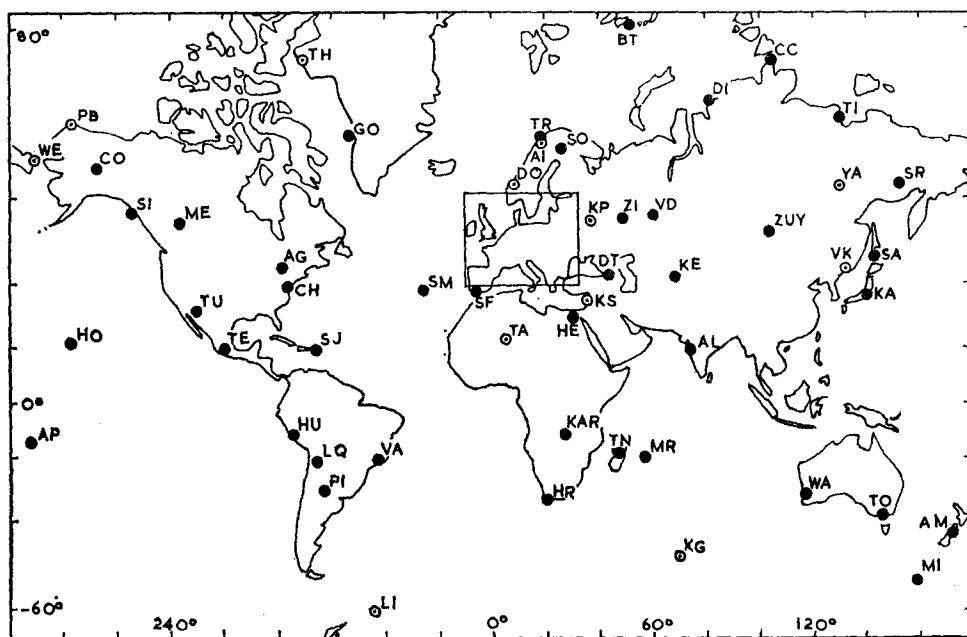

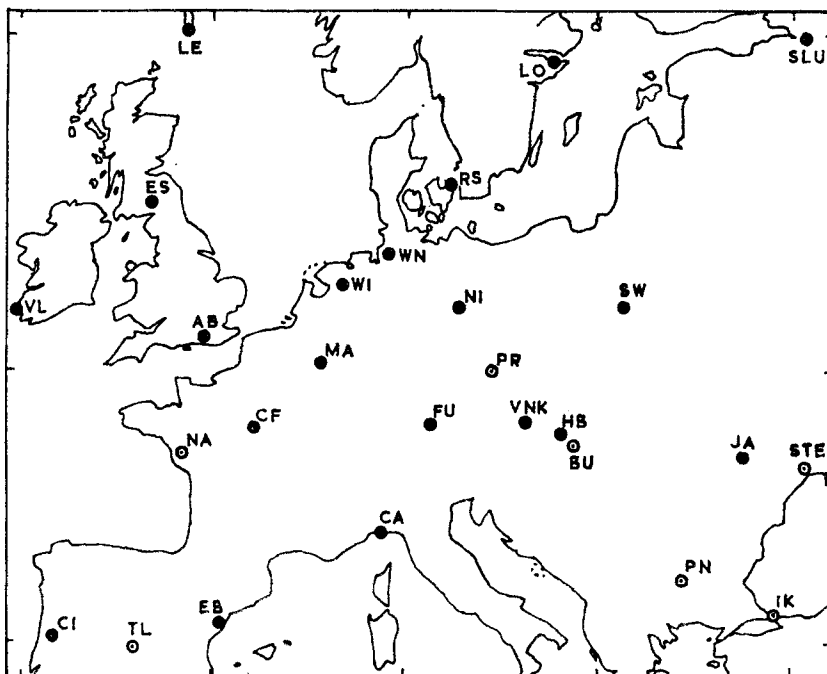FIG. 1. Observatories used in the analysis.

FIG. 2. Observatories used in the analysis (Europe).

necessary so that the mean epoch was equal to the epoch required. In cases where the first three or last three values were missing, the value nearest to the required epoch was corrected to that epoch using a value for secular variation deduced from the other annual mean values for that observatory; in no case was reference made to secular variation from any other source.

In order to keep the data from any one observatory as homogeneous as possible, discontinuities introduced by a change of standard or of site were removed. Where a change of site occurred, all the data were corrected to the site with the longest run of data.

So that the analyses for each epoch should be strictly comparable it was important that the same set of observatories should be used for each analysis. There were 62 observatories for which X, Y and Z data were available and one observatory (Yakutsk) for which X and Y data were available for all five epochs. To increase this number and improve the geographical distribution of data it was necessary to estimate missing values. This was done only for observatories where there were four epochs for which a value of the required element existed. A smooth curve was drawn through the existing values of the element and the value at the required epoch was read off. In this manner the Z data for Yakutsk and X, Y and Z data for a further 17 observatories were available for the analysis, making a total of 80 complete observatories.

The positions of these 80 observatories are shown in Figs 1 and 2. Filled circles indicate observatories for which the data are complete, open circles indicate observatories where the values for one epoch have been estimated. The abbreviations used are those in IAGA Bulletin No. 20 except for four observatories which do not appear in this bulletin. These observatories and their abbreviations are Helwan, HE; Abinger, AB; Cheltenham, CH and Jassy, JA. As with most geomagnetic work, the distribution leaves much to be desired, having a dense coverage over Europe and a very sparse coverage in the southern hemisphere.

The five year means are listed in Table 1, with the observatories in order of co-latitude. Estimated values are in italics

3. The analysis

The geomagnetic potential, V, was assumed to satisfy Laplace's equation and to be of purely internal origin so that it could be represented by

$$V = R \sum_{n=1}^{k} \sum_{m=0}^{n} (g_n^m \cos m\lambda + h_n^m \sin m\lambda) \left(\frac{R}{r}\right)^{n+1} P_n^m(\cos\theta) \tag{1}$$

where g_n^m, h_n^m are spherical harmonic coefficients.

θ, λ and r are spherical co-ordinates measured respectively from the north geographical pole, the Greenwich meridian (east positive) and the centre of the Earth.

R is the radius of a reference sphere chosen to be equal to the mean radius of the Earth (6371·2 km). For all the observatories r was taken to be equal to R.

$P_n^m(\cos\theta)$ are the associated Legendre polynomials in the Schmidt quasi-normalized form.

The order of the analysis, k, was chosen to be 6. This value implies 48 spherical harmonic coefficients, which is a reasonable number to deduce from data from 80 positions. Also it has been shown that, at least for the main field, a very good fit to the data is obtained with a sixth order analysis, which is not greatly improved upon even by a ninth order analysis using twice the number of coefficients (Malin & Pocock 1969). A possible explanation for this is that the first six orders represent most of the deep seated part of the field, while the higher orders are more representative of shallow anomalies, which are not fitted so efficiently with a centred function. It is the deep seated part of the field which is required, since this is thought to be the source of secular variation.

Each observed element at each observatory gave an equation of condition in the 48 spherical harmonic coefficients, making a total of 240 equations for each epoch. From these equations values of g_n^m and h_n^m were derived by the method of least squares.

Since the same set of observatories was used throughout, the coefficients of g_n^m and h_n^m in the equations of conditions were the same for each epoch, so the normal equations matrix remained the same. Thus it was only necessary to invert one matrix. Further, since the equations were linear in g_n^m and h_n^m, differencing successive epochs of g_n^m and h_n^m yielded the same values for secular variation coefficients, $\dot{g}_n^m$ and $\dot{h}_n^m$, as would an analysis of differences between successive epochs of X, Y and Z at the observatories.

Standard deviations of the coefficients were deduced from S, the sum of the squares of the residuals from the initial data and W_n^m, the weights of the unknowns as indicated by the coefficients of the leading diagonal of the inverse of the normal equation matrix:

$$\text{standard deviation} = \left(\frac{S \cdot W_n^m}{3 \times 80 - 48}\right)^{\frac{1}{2}}.$$

(The denominator is equal to the number of equations of condition *minus* the number of unknowns.)

Thus five sets of main field coefficients, four sets of secular variation coefficients and the associated standard deviations were derived (Tables 2 and 3). No special

Table 1

Observatory	Latitude	Longitude E	1942.5 X γ	Y γ	Z γ	1947.5 X γ	Y γ	Z γ	1952.5 X γ	Y γ	Z γ	1957.5 X γ	Y γ	Z γ	1962.5 X γ	Y γ	Z γ
BT	80° 20′	52° 48′	5829	2509	54713	5688	2571	54846	5568	2680	54944	5498	2711	55066	5415	2695	55199
CC	77 43	104 17	3433	1595	58028	3292	1546	58143	3147	1432	58324	3091	1343	58512	3109	1236	58733
TH	76 32	290 56	866	−4387	55696	937	−4336	55761	1008	−4285	55826	1076	−4227	55938	1140	−4162	56098
DI	73 33	80 34	5921	3255	56964	5740	3260	57154	5589	3283	57413	5519	3234	57651	5525	3180	57897
TI	71 35	129 00	7229	−1495	59134	7152	−1577	59409	7074	−1766	59324	7106	−1925	59444	7230	−2038	59546
PB	71 18	203 15	8234	4265	56163	8338	4240	56266	8445	4215	56370	8535	4203	56406	8636	4203	56386
TR	69 40	18 57	11235	−426	50428	11169	−283	50570	11150	−147	50704	11183	−51	50861	11215	1	51034
GO	69 14	306 29	4717	−6663	55136	4817	−6594	55076	4900	−6535	55146	5006	−6488	55273	5102	−6445	55478
AI	68 22	18 49	11692	−8	49889	11613	144	50026	11599	288	50143	11620	393	50332	11674	503	50448
SO	67 22	26 38	11830	892	49489	11739	1019	49650	11709	1156	49789	11718	1257	49961	11751	1307	50121
WE	66 10	190 10	13223	3683	53473	13286	3617	53554	13349	3552	53634	13411	3537	53556	13538	3537	53562
CO	64 52	212 10	10933	6218	55423	10962	6167	55332	11035	6153	55395	11118	6141	55359	11219	6139	55335
SR	62 26	152 19	16180	−2547	53908	16173	−2706	54025	16208	−2872	54165	16301	−2976	54256	16431	−3006	54313
DO	62 04	9 07	13875	−1611	47148	13815	−1440	47332	13811	−1293	47500	13870	−1179	47650	13952	−1102	47791
YA	62 01	129 43	13860	−4323	57969	13806	−4457	58130	13796	−4630	58281	13886	−4765	58420	14050	−4870	58432
LE	60 08	358 49	14074	−2959	46901	14099	−2779	47000	14177	−2628	47084	14271	−2507	47218	14385	−2423	47339
SLU	59 57	30 42	15058	1437	47860	14925	1560	48141	14908	1704	48208	14909	1801	48404	14949	1838	48555
LO	59 21	17 50	15287	−326	46881	15223	−158	47049	15225	5	47193	15248	124	47344	15302	196	47489
SI	57 03	224 40	13461	7668	55035	13507	7612	55020	13562	7574	54965	13648	7540	54954	13757	7517	54893
VD	56 44	61 04	15645	3612	51247	15549	3667	51535	15497	3749	51822	15497	3781	52073	15552	3762	52216
RS	55 51	12 27	16680	−1199	45241	16651	−1006	45411	16683	−829	45547	16728	−689	45680	16799	−591	45813
ZI	55 50	48 51	16381	2752	48932	16277	2826	49192	16235	2925	49443	16229	2985	49662	16272	2987	49790
KP	55 29	37 19	17054	2017	47540	17010	2139	47741	16968	2259	47938	16954	2337	48138	16989	2355	48294
ES	55 19	356 48	16113	−3621	45059	16172	−3425	45145	16286	−3255	45213	16410	−3110	45297	16556	−2997	45398
ME	54 37	246 40	11479	5492	59185	11585	5418	59216	11691	5368	59013	11772	5324	58785	11916	5316	58730
WN	53 45	9 04	17542	−1704	44213	17544	−1494	44381	17597	−1307	44499	17659	−1155	44626	17746	−1041	44749
WI	52 49	6 40	17831	−2142	43745	17852	−1918	43889	17932	−1729	44022	18011	−1565	44149	18113	−1445	44262
ZUY	52 28	104 02	19012	−212	56891	19002	−297	57267	19007	−402	57570	19081	−520	57718	19189	−634	57709
SW	52 07	21 15	18292	−124	44295	18230	53	44540	18230	227	44718	18250	361	44922	18289	444	45078
NI	52 04	12 40	18385	−1252	43518	18360	−1044	43683	18400	−852	43825	18451	−696	43979	18525	−583	44112
VL	51 56	349 45	17181	−4755	43966	17288	−4557	44019	17477	−4412	44160	17684	−4275	44180	17881	−4150	44246
AB	51 11	359 37	18244	−3354	43147	18317	−3138	43243	18438	−2948	43312	18568	−2780	43395	18743	−2643	43463
MA	50 18	5 41	18959	−2365	42733	18982	−2150	42887	19091	−1944	43008	19186	−1758	43138	19287	−1624	43248
PR	49 59	14 33	19366	−994	42494	19410	−802	42670	19455	−610	42850	19497	−447	42999	19559	−316	43143
VNK	48 16	16 19	20427	−832	41716	20411	−616	41979	20431	−414	42183	20473	−254	42351	20535	−137	42481
FU	48 10	11 17	20230	−1584	41467	20250	−1353	41664	20312	−1139	41813	20373	−962	41948	20455	−822	42064
CF	48 01	2 16	19838	−2995	41557	19911	−2757	41677	20024	−2540	41747	20148	−2350	41844	20287	−2198	41924
HB	47 52	18 11	20660	−603	41597	20612	−387	41741	20664	−192	41995	20693	−35	42190	20749	75	42340
BU	47 31	18 54	20821	−517	41441	20815	−301	41664	20807	−84	41890	20843	74	42065	20904	185	42225
NA	47 15	358 26	20004	−3583	41102	20117	−3344	41272	20273	−3133	41499	20438	−2931	41558	20583	−2747	41710

Table 1 (*continued*)

Observatory	Latitude	Longitude E.	1942.5 X γ	1942.5 Y γ	1942.5 Z γ	1947.5 X γ	1947.5 Y γ	1947.5 Z γ	1952.5 X γ	1952.5 Y γ	1952.5 Z γ	1957.5 X γ	1957.5 Y γ	1957.5 Z γ	1962.5 X γ	1962.5 Y γ	1962.5 Z γ
JA	47° 11′	27° 32′	21325	548	41966	21293	716	42410	21286	852	42765	21240	1040	42730	21251	1068	42818
SA	46 57	142 43	24813	−4100	44700	24870	−4211	44882	24960	−4379	44953	25031	−4463	44930	25122	−4488	44798
STE	46 47	30 53	21310	367	42272	21302	484	42525	21296	600	42778	21275	691	42976	21283	743	43118
CA	44 26	8 56	22053	−2259	38890	22125	−2007	39123	22209	−1767	39277	22298	−1563	39416	22411	−1403	39611
AG	43 47	280 44	15169	−2003	56462	15210	−1975	56332	15329	−1960	56222	15519	−1989	56204	15792	−2043	56147
VK	43 47	132 02	26521	−4047	45449	26528	−4133	45496	26554	−4204	45510	26590	−4268	45507	26665	−4303	45437
PN	42 31	24 11	23410	−137	38494	23438	58	38743	23468	253	38995	23476	396	39195	23521	486	39384
DT	42 06	44 42	24055	2098	40933	24029	2128	41306	24045	2182	41623	24052	2210	41871	24083	2178	42033
KE	41 25	69 12	25365	2280	44659	25470	2255	44999	25572	2267	45322	25650	2227	45539	25727	2169	45630
IK	41 04	29 04	24667	708	37796	24699	861	38216	24731	1014	38646	24751	1121	38900	24791	1188	39098
EB	40 49	0 30	23357	−3533	36725	23488	−3267	36879	23666	−3020	36878	23831	−2788	36896	23994	−2577	36878
CI	40 13	351 35	22862	−4981	36491	23075	−4748	36656	23317	−4519	36818	23530	−4293	36778	23757	−4091	36731
TL	39 53	355 57	23400	−4294	36296	23602	−4050	36272	23806	−3807	36247	24003	−3572	36228	24208	−3351	36204
CH	38 44	283 10	18040	−2245	53923	18090	−2247	53853	18256	−2275	53799	18450	−2361	53686	18707	−2466	53460
SM	37 46	334 .21	22535	−7074	39460	22798	−6953	39247	23163	−6839	39078	23511	−6724	38872	23887	−6581	38658
SF	36 28	353 48	24962	−4874	33678	25146	−4604	33633	25387	−4360	33549	25605	−4096	33452	25844	−3841	33282
KA	36 14	140 11	29642	−3138	34901	29738	−3237	35001	29870	−3330	35048	29938	−3353	35000	29985	−3363	34874
KS	33 49	35 53	28701	1036	32421	28774	1121	32820	28844	1214	33131	28919	1286	33426	28992	1369	33715
TU	32 15	249 10	25355	6211	44602	25311	6117	44379	25294	6017	44168	25252	5955	43978	25227	5892	43764
HE	29 52	31 20	30504	303	27709	30628	427	28068	30733	550	28349	30867	665	28610	30955	757	28791
TA	22 48	5 32	31545	−3934	17968	31727	−3617	17916	31952	−3338	17867	32112	−3042	17821	32301	−2744	17778
HO	21 18	201 54	28187	5740	22915	28087	5757	22922	27937	5749	23024	27835	5725	22990	27752	5724	22920
TE	19 45	260 49	30317	5170	33164	30152	5080	32873	30079	4911	32745	29882	4803	32630	29716	4651	32443
AL	18 38	72 52	37935	−390	17836	38230	−462	17759	38483	−478	17731	38627	−531	17723	38732	−602	17656
SJ	18 23	293 53	27179	−2842	35958	27270	−3014	35688	27369	−3201	35244	27407	−3454	34724	27408	−3710	34134
KAR	−11 40	27 28	23089	−3676	−24844	22948	−3582	−24883	22798	−3502	−24882	22621	−3401	−24950	22413	−3229	−25096
HU	−12 03	284 40	29224	3460	1135	29029	3237	1062	28773	2995	1002	28514	2716	991	28254	2435	1040
AP	−13 48	188 14	34246	6672	−20639	34208	6828	−20588	34185	7028	−20446	34140	7108	−20383	34051	7197	−20356
TN	−18 55	47 33	20749	−3598	−28807	20546	−3824	−28764	20296	−3996	−28611	20114	−4160	−28509	19994	−4278	−28419
MR	−20 06	57 33	21714	−5549	−29970	21573	−5854	−30235	21450	−6135	−30475	21358	−6300	−30525	21293	−6440	−30483
LQ	−22 06	294 24	25833	1557	−5923	25565	1265	−6053	25278	1012	−6144	24987	721	−6176	24691	389	−6165
VA	−22 24	316 21	22888	−5703	−8149	22547	−5856	−8460	22169	−6027	−8839	21774	−6217	−9223	21396	−6417	−9601
WA	−30 19	115 53	24673	−1353	−51611	24771	−1251	−51878	24830	−1210	−52112	24831	−1168	−52210	24823	−1164	−52238
PI	−31 40	296 07	23905	2176	−12051	23566	1944	−12064	23212	1704	−12062	22905	1439	−12026	22610	1146	−11930
HR	−34 25	19 14	12974	−5729	−29160	12638	−5570	−28730	12314	−5443	−28277	11978	−5343	−27874	11627	−5216	−27442
TO	−37 32	145 28	22584	3563	−56179	22546	3697	−56255	22461	3854	−56406	22362	3987	−56418	22242	4074	−56399
AM	−43 09	172 43	21063	7111	−55210	20957	7301	−55207	20851	7520	−55160	20734	7667	−55066	20592	7797	−54941
KG	−49 33	69 49	12400	−13000	−42765	12199	−13338	−43225	12036	−13675	−43900	11879	−13965	−44178	11595	−14203	−44606
MI	−54 30	158 57	12541	5138	−64802	12373	5300	−64684	12200	5446	−64556	12058	5640	−64470	11882	5785	−64336
LI	−60 44	315 13	23190	1047	−32146	22827	954	−31609	22478	879	−31159	22107	811	−30652	21746	749	−30121

Table 2

Spherical harmonic coefficients for the main geomagnetic field

g, h	n	m	1942.5 γ	1947.5 γ	1952.5 γ	1957.5 γ	1962.5 γ
g	1	0	−30707·6 ± 39·2	−30674·1 ± 38·4	−30643·8 ± 38·9	−30583·4 ± 39·2	−30501·4 ± 40·5
g	1	1	−2339·3 44·9	−2293·2 44·1	−2233·1 44·6	−2189·2 44·9	−2139·5 46·4
h	1	1	5726·2 45·9	5739·4 45·0	5742·3 45·5	5738·0 45·9	5740·7 47·4
g	2	0	−1089·7 38·0	−1186·4 37·3	−1283·3 37·8	−1387·4 38·0	−1498·3 39·3
g	2	1	2980·4 35·4	2982·2 34·7	2983·6 35·1	2985·2 35·4	2981·6 36·5
h	2	1	−1581·9 40·2	−1690·5 39·5	−1795·2 39·9	−1874·4 40·2	−1949·5 41·5
g	2	2	1587·1 42·7	1586·0 41·9	1581·4 42·4	1587·8 42·7	1604·1 44·1
h	2	2	461·6 45·2	382·0 44·3	286·4 44·9	196·6 45·2	110·1 46·7
g	3	0	1125·2 31·7	1151·0 31·1	1171·9 31·4	1180·3 31·7	1177·3 32·7
g	3	1	−1782·8 27·6	−1841·2 27·1	−1901·6 27·4	−1958·2 27·6	−2014·2 28·5
h	3	1	−490·1 36·9	−478·2 36·2	−452·6 36·6	−428·8 36·9	−391·7 38·1
g	3	2	1264·5 26·8	1281·7 26·3	1306·7 26·6	1316·9 26·8	1317·5 27·7
h	3	2	188·0 32·2	203·1 31·5	219·6 31·9	225·8 32·2	228·8 32·2
g	3	3	872·5 34·4	856·8 33·7	847·0 34·1	839·9 34·4	827·4 35·5
h	3	3	73·9 33·6	33·8 32·9	8·8 33·3	−37·0 33·6	−77·4 34·7
g	4	0	940·3 32·0	942·0 31·4	944·2 31·8	942·3 32·0	933·2 33·1
g	4	1	773·0 25·9	791·4 25·4	796·0 25·7	801·4 25·9	806·7 26·7
h	4	1	173·8 29·9	167·0 29·3	156·4 29·7	146·5 29·9	144·7 30·9
g	4	2	552·5 24·3	534·8 23·8	513·0 24·1	493·5 24·3	464·0 25·1
h	4	2	−241·3 30·1	−238·6 29·5	−228·9 29·8	−221·6 30·1	−214·6 31·0
g	4	3	−399·2 26·0	−386·3 25·5	−377·8 25·9	−372·7 26·0	−363·2 26·9
h	4	3	−35·0 23·2	−16·0 22·7	2·6 23·0	16·8 23·2	31·5 24·0
g	4	4	241·4 32·0	254·7 31·4	251·1 31·8	239·9 32·0	232·7 33·1
h	4	4	−139·7 31·5	−166·4 30·9	−198·3 31·3	−211·1 31·5	−223·6 32·5

Table 2 (*continued*)

g,h	n	m	1942.5 γ		1947.5 γ		1952.5 γ		1957.5 γ		1962.5 γ	
g	5	0	−309·5±29·0		−292·7±28·5		−277·2±28·8		−266·8±29·0		−254·8±30·0	
g	5	1	292·1	24·1	306·2	23·7	319·9	23·9	326·2	24·1	329·5	24·9
h	5	1	−21·8	25·4	−4·2	24·9	12·7	25·2	32·3	25·4	45·0	26·2
g	5	2	182·1	22·1	201·5	21·6	224·8	21·9	245·9	22·1	270·6	22·8
h	5	2	123·3	24·7	118·4	24·3	117·4	24·6	126·1	24·7	130·9	25·5
g	5	3	36·6	28·8	35·9	28·3	31·5	28·6	32·0	28·8	24·5	29·8
h	5	3	−61·0	24·2	−79·7	23·7	−97·6	24·0	−108·0	24·2	−122·9	25·0
g	5	4	−180·3	24·6	−186·0	24·1	−194·0	24·4	−198·1	24·5	−202·7	25·4
h	5	4	−85·5	23·6	−85·7	23·1	−77·6	23·4	−71·7	23·6	−63·6	24·4
g	5	5	−120·9	30·2	−113·3	29·6	−105·3	30·0	−102·6	30·2	−96·1	31·2
h	5	5	66·0	30·1	58·6	29·5	50·2	29·9	48·4	30·1	47·7	31·1
g	6	0	158·4	19·3	150·5	18·9	142·3	19·1	137·6	19·3	133·6	19·9
g	6	1	47·6	17·7	43·9	17·4	44·5	17·6	44·6	17·7	45·6	18·3
h	6	1	−56·7	17·4	−64·1	17·1	−68·6	17·3	−80·5	17·4	−90·8	18·0
g	6	2	19·4	17·3	15·3	16·9	9·4	17·1	8·1	17·3	10·2	17·8
h	6	2	52·4	18·4	56·4	18·1	60·7	18·3	61·8	18·4	67·7	19·0
g	6	3	−296·1	19·4	−300·5	19·0	−292·9	19·2	−287·4	19·4	−277·1	20·0
h	6	3	21·0	16·4	35·3	16·1	54·5	16·3	67·0	16·4	79·3	17·0
g	6	4	26·7	21·3	31·0	20·8	37·9	21·1	42·5	21·3	44·4	22·0
h	6	4	−59·1	20·9	−62·7	20·5	−72·9	20·8	−83·6	20·9	−93·9	21·6
g	6	5	50·7	17·8	41·2	17·5	36·1	17·7	31·3	17·8	27·4	18·4
h	6	5	−2·4	19·5	−1·6	19·1	−1·1	19·3	−0·3	19·5	−0·3	20·1
g	6	6	−102·8	28·4	−100·3	27·8	−92·8	28·1	−92·4	28·3	−94·4	29·3
h	6	6	40·0	28·4	50·3	27·8	60·8	28·2	65·6	28·4	73·6	29·3

Table 3

Spherical harmonic coefficients for the secular variation field

g, h	n	m	1942.5 to 1947.5 γ yr^{-1}		1947.5 to 1952.5 γ yr^{-1}		1952.5 to 1957.5 γ yr^{-1}		1957.5 to 1962.5 γ yr^{-1}		1942.5 to 1962.5 γ yr^{-1}	
g	1	0	6·7±1·3		6·1±1·4		12·1±0·9		16·4±1·0		10·3±0·7	
g	1	1	9·2	1·5	12·0	1·7	8·8	1·1	9·9	1·1	10·0	0·8
h	1	1	2·6	1·5	0·6	1·7	−0·9	1·1	0·5	1·1	0·7	0·8
g	2	0	−19·3	1·2	−19·4	1·4	−20·8	0·9	−22·2	0·9	−20·4	0·7
g	2	1	0·4	1·2	0·3	1·3	0·3	0·8	−0·7	0·9	0·1	0·6
h	2	1	−21·7	1·3	−20·9	1·5	−15·8	1·0	−15·0	1·0	−18·4	0·7
g	2	2	−0·2	1·4	−0·9	1·6	1·3	1·0	3·3	1·0	0·8	0·8
h	2	2	−15·9	1·5	−19·1	1·7	−18·0	1·1	−17·3	1·1	−17·6	0·8
g	3	0	5·2	1·0	4·2	1·2	1·7	0·8	−0·6	0·8	2·6	0·6
g	3	1	−11·7	0·9	−12·1	1·0	−11·3	0·7	−11·2	0·7	−11·6	0·5
h	3	1	2·4	1·2	5·1	1·4	4·8	0·9	7·4	0·9	4·9	0·7
g	3	2	3·4	0·9	5·0	1·0	2·0	0·6	0·1	0·7	2·6	0·5
h	3	2	3·0	1·1	3·3	1·2	1·2	0·8	0·6	0·8	2·0	0·6
g	3	3	−3·1	1·1	−2·0	1·3	−1·4	0·8	−2·5	0·8	−2·3	0·6
h	3	3	−8·0	1·1	−5·0	1·2	−9·2	0·8	−8·1	0·8	−7·6	0·6
g	4	0	0·3	1·0	0·4	1·2	−0·4	0·8	−1·8	0·8	−0·4	0·6
g	4	1	3·7	0·8	0·9	1·0	1·1	0·6	1·1	0·6	1·7	0·5
h	4	1	−1·4	1·0	−2·1	1·1	−2·0	0·7	−0·4	0·7	−1·5	0·5
g	4	2	−3·5	0·8	−4·4	0·9	−3·9	0·6	−5·9	0·6	−4·4	0·4
h	4	2	0·5	1·0	1·9	1·1	1·5	0·7	1·4	0·7	1·3	0·5
g	4	3	2·6	0·9	1·7	1·0	1·0	0·6	1·9	0·6	1·8	0·5
h	4	3	3·8	0·8	3·7	0·9	2·8	0·6	2·9	0·6	3·3	0·4
g	4	4	2·7	1·0	−0·7	1·2	−2·2	0·8	−1·4	0·8	−0·4	0·6
h	4	4	−5·3	1·0	−6·4	1·2	−2·6	0·7	−2·5	0·8	−4·2	0·6
g	5	0	3·4	1·0	3·1	1·1	2·1	0·7	2·4	0·7	2·7	0·5
g	5	1	2·8	0·8	2·7	0·9	1·3	0·6	0·7	0·6	1·9	0·4
h	5	1	3·5	0·8	3·4	0·9	3·9	0·6	2·5	0·6	3·3	0·5
g	5	2	3·9	0·7	4·7	0·8	4·2	0·5	4·9	0·5	4·4	0·4
h	5	2	−1·0	0·8	−0·2	0·9	1·7	0·6	1·0	0·6	0·4	0·4
g	5	3	−0·1	0·9	−0·9	1·1	0·1	0·7	−1·5	0·7	−0·6	0·5
h	5	3	−3·7	0·8	−3·6	0·9	−2·1	0·6	−3·0	0·6	−3·1	0·4
g	5	4	−1·1	0·8	−1·6	0·9	−0·8	0·6	−0·9	0·6	−1·1	0·4
h	5	4	0·0	0·8	1·6	0·9	1·2	0·6	1·6	0·6	1·1	0·4
g	5	5	1·5	1·0	1·6	1·1	0·5	0·7	1·3	0·7	1·2	0·5
h	5	5	−1·5	1·0	−1·7	1·1	−0·4	0·7	−0·1	0·7	−0·9	0·5
g	6	0	−1·6	0·6	−1·6	0·7	−0·9	0·5	−0·8	0·5	−1·2	0·3
g	6	1	−0·7	0·6	0·1	0·7	0·0	0·4	0·2	0·4	−0·1	0·3
h	6	1	−1·5	0·6	−0·9	0·6	−2·4	0·4	−2·1	0·4	−1·7	0·3
g	6	2	−0·8	0·6	−1·2	0·6	−0·3	0·4	0·4	0·4	−0·5	0·3
h	6	2	0·8	0·6	0·9	0·7	0·2	0·4	1·2	0·4	0·8	0·3
g	6	3	−0·9	0·6	1·5	0·7	1·1	0·5	2·1	0·5	1·0	0·3
h	6	3	2·9	0·5	3·8	0·6	2·5	0·4	2·5	0·4	2·9	0·3
g	6	4	0·9	0·7	1·4	0·8	0·9	0·5	0·4	0·5	0·9	0·4
h	6	4	−0·7	0·7	−2·0	0·8	−2·1	0·5	−2·1	0·5	−1·7	0·4
g	6	5	−1·9	0·6	−1·0	0·7	−1·0	0·4	−0·8	0·4	−1·2	0·3
h	6	5	0·2	0·6	0·1	0·7	0·2	0·5	0·0	0·5	0·1	0·4
g	6	6	0·5	0·9	1·5	1·0	0·1	0·7	−0·4	0·7	0·4	0·5
h	6	6	2·1	0·9	2·1	1·0	1·0	0·7	1·6	0·7	1·7	0·5

merit is claimed for the main field coefficients, although Fougère (1965) has shown
that a reasonably good model can be derived from annual mean values of X, Y and
Z from about 80 observatories. However, the secular variation coefficients and,
more particularly, variations of the secular variation coefficients with time, should
be well determined.

4. Secular variation

Charts of mean secular variation of X, Y and Z for the interval 1942.5 to 1962.5
deduced from the coefficients in Table 3 are shown in Figs 3, 4 and 5. The charts
are on Mercator's projection and extend from 80° N to 80° S. Contours are drawn
at intervals of $20\,\gamma\,\mathrm{yr}^{-1}$ with positive and zero values shown by solid lines and negative
values shown by broken lines.

It is of interest to compare these charts with the following four sets of charts,
which are also based on observatory annual mean data:

   (i) Leaton (1962) for the epoch 1955,

  (ii) Negata & Syono (1961) for the period from 1955 to 1960,

 (iii) Orlov (1965) for the epoch 1965, and

  (iv) Leaton, Malin & Evans (1965) for the epoch 1965.

The charts for (iv) are published separately by the British Admiralty.

On the $\dot{X}$ chart the most prominent feature in all cases is the deep negative focus
in the South Atlantic. The present analysis centres this focus at 40° S, 340° E with
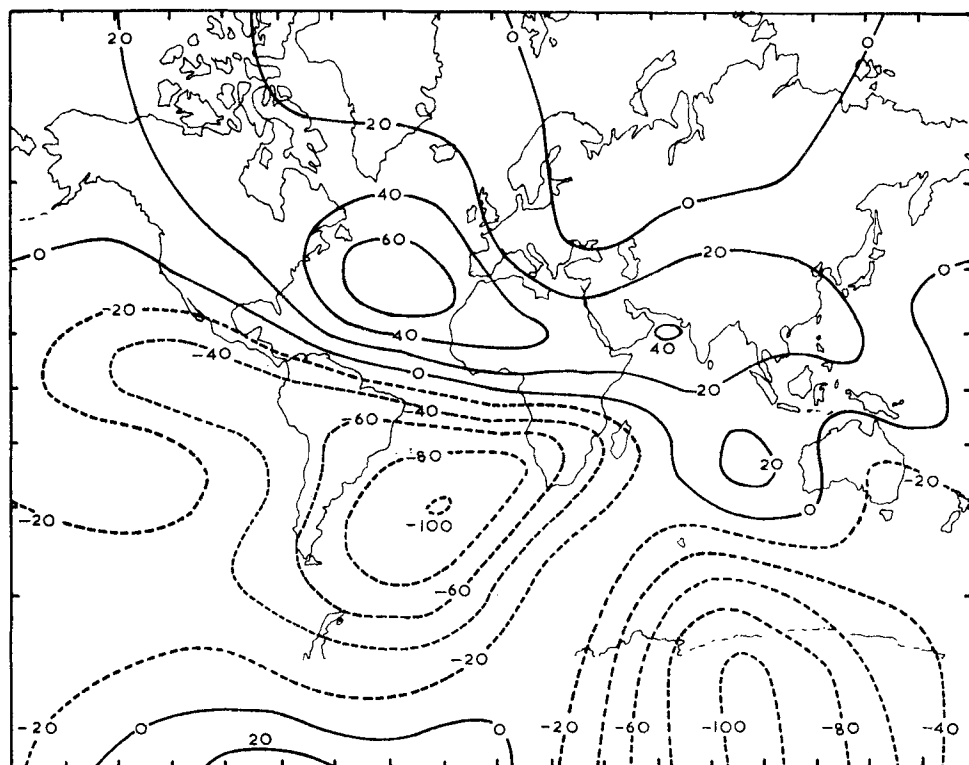
FIG. 3. Secular variation in X in units of $\gamma\,\mathrm{yr}^{-1}$.
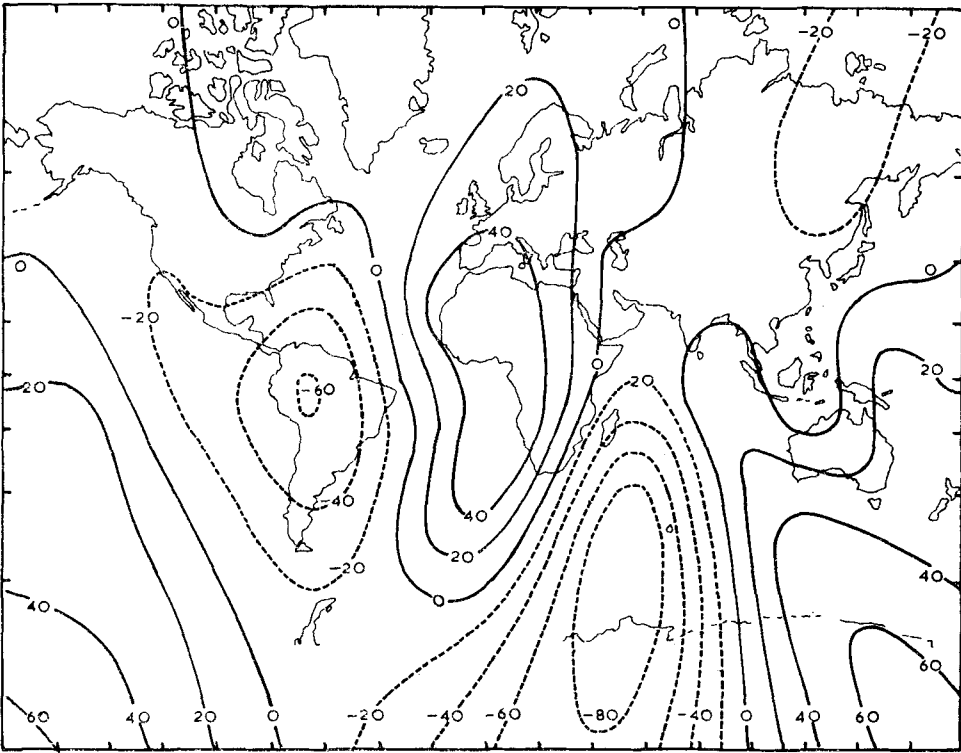
FIG. 4. Secular variation in Y in units of $\gamma\,\mathrm{yr}^{-1}$.

a value of $-100\,\gamma\,\mathrm{yr}^{-1}$. The other authors vary between 40° S and 45° S, 333° E and 339° E, $-95\,\gamma\,\mathrm{yr}^{-1}$ and $-110\,\gamma\,\mathrm{yr}^{-1}$, but no systematic change with time is discernible. There is also a region of large negative change near the south magnetic pole, reaching $-100\,\gamma\,\mathrm{yr}^{-1}$ at 80° S, 99° E. (ii) and (iii) show a similar feature, but (i) shows a value of $-80\,\gamma\,\mathrm{yr}^{-1}$ at 120° E. The only deep positive focus $(72\,\gamma\,\mathrm{yr}^{-1})$ occurs at 40° N, 320° E. (i) and (iv) agree with this position although (iv) gives a value of $90\,\gamma\,\mathrm{yr}^{-1}$. (ii) places the focus at 45° N, 315° E with a value of $80\,\gamma\,\mathrm{yr}^{-1}$ and (iii) places it at 50°N, 325°E with a value of $60\,\gamma\,\mathrm{yr}^{-1}$. All sources show a small negative value over most of the Pacific and a small positive value over most of the U.S.S.R.

The $\dot{Y}$ chart (Fig. 4) shows four main foci, two positive and two negative, which divide the world into four segments of longitude of alternate sign. The negative foci are centred in South America $(-60\,\gamma\,\mathrm{yr}^{-1})$ and the South Indian Ocean $(-90\,\gamma\,\mathrm{yr}^{-1})$. One of the positive foci is elongated along the Greenwich meridian $(58\,\gamma\,\mathrm{yr}^{-1})$ and the other is connected with the singular point at the geographical South Pole, where it attains a value of $72\,\gamma\,\mathrm{yr}^{-1}$ in the direction 190° E. All of the other authors show a similar pattern, but there are differences in detail. (iii) and (iv) agree with the present value for the Greenwich meridian focus, but (iii) places it further west in central Africa. (i) and (ii) show a larger rate of change $(70\,\gamma\,\mathrm{yr}^{-1})$, but differ from each other by 40° in the latitude of the maximum. There is some divergence of opinion over the South Indian Ocean focus, probably because of the shortage of data in this region. Estimates of its centre vary between 50° S and 80° S, 35° E and 70° E, which bracket the present estimate; however, the other sources all have a lower intensity with (iii) and (iv) both around $-55\,\gamma\,\mathrm{yr}^{-1}$. There is some confusion over the maximum at the south polar discontinuity. (i) shows a value of $80\,\gamma\,\mathrm{yr}^{-1}$ at 190° E, but this is
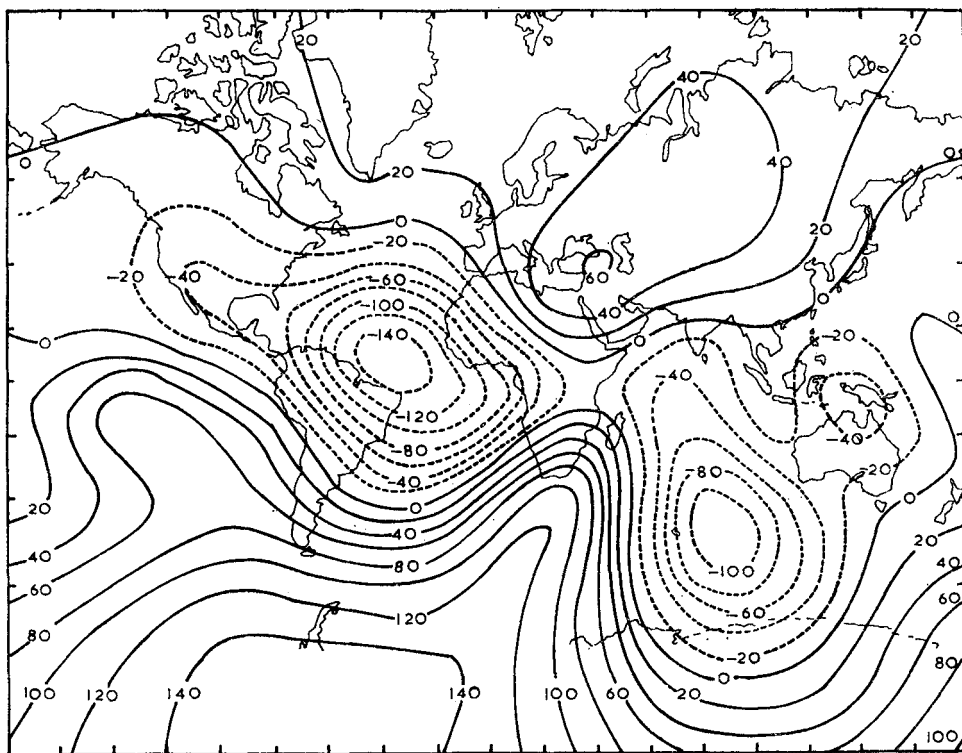
FIG. 5. Secular variation in Z in units of $\gamma\ yr^{-1}$.

incompatible with the $\dot{H}$ value of $70\gamma\ yr^{-1}$ at the South Pole. By implication (ii) shows a value of $60\gamma\ yr^{-1}$ (since the negative lobe of the singularity reaches this amplitude). (iii) erroneously shows no singularity at all. (iv) does not show the polar regions. There is no significant disagreement over the South American focus.

The secular variation in Z (Fig. 5) is more extreme than in X and Y, with deeper foci and steeper gradients. There are three foci where the rate of change exceeds $100\gamma\ yr^{-1}$; one positive in the Antarctic (80° S, 285° E, $153\gamma\ yr^{-1}$) and two negative, the first in the central Atlantic (10° N, 320° E, $-155\gamma\ yr^{-1}$) and the second in the South Indian Ocean (50° S, 90° E, $-113\gamma\ yr^{-1}$). Over most of Europe, Asia and the Artic the value is small and positive, with a $60\gamma\ yr^{-1}$ focus in East Turkey. (i) and (ii) are in good agreement with this picture, although (i) has a rather shallower Indian Ocean focus $(-70\gamma\ yr^{-1})$ and (ii) shows the Antarctic focus rising to $200\gamma\ yr^{-1}$ near the South Pole. This feature is also shown by (iii) ($170\gamma\ yr^{-1}$). The only direct evidence for a deep focus in Antarctica was the $\dot{Z}$ value of $181\gamma\ yr^{-1}$ deduced from the 1957–59 observations at Syowa. No other Antarctic station had a value greater than $132\gamma\ yr^{-1}$. More recent data (*Royal Observatory Bulletin* p. 134, 1967) show that the Syowa $\dot{Z}$ values are rather erratic, but have a mean value of $106\gamma\ yr^{-1}$; they also confirm that no observatory shows a value greater than $140\gamma\ yr^{-1}$. The other three foci are also shown by (iii), but with slightly lower amplitudes. (iv) shows considerable differences. No European focus is shown, the Indian Ocean focus is moved north-east to 15° S, 97° E, a new focus appears in the central Pacific (0°, 220° E, $-65\gamma\ yr^{-1}$) and the Antarctic focus divides into two (60° S, 240° E, $175\gamma\ yr^{-1}$; 50° S, 32° E, $150\gamma\ yr^{-1}$).

In addition to the sources already mentioned, there is a $\dot{Z}$ chart prepared by the United States Coast and Geodetic Survey for the epoch 1965. The data used for this

chart included observatory annual means, repeat station values and observations from successive surveys. The Atlantic focus is shown to the north-west of the present determination and considerably deeper (21° N, 313° E, $-205\,\gamma\,\mathrm{yr}^{-1}$), the Indian Ocean and European foci are in quite good agreement with the present estimates, but, as in the case of (iv), the Antarctic focus is divided into two (70° S, 230° E, $165\,\gamma\,\mathrm{yr}^{-1}$; 55° S, 42° E, $102\,\gamma\,\mathrm{yr}^{-1}$).

For those estimates of secular variation which are products of, or have been subjected to spherical harmonic analysis, their differences may be discussed in terms of the departures of their spherical harmonic coefficients from those obtained in the present analysis. For this comparison (i), (ii), (iv), cited above, plus (v) Adam, Benkova, Orlov, Osipov & Tiurmina (1963) for the interval 1954 to 1959 and (vi) Cain (1966) for the epoch 1960, were considered. The analysis of Cain differs slightly from the others in that the results are much more dependent on survey data than on observatory data and allowance was made for the oblateness of the Earth. The departures of coefficients of the above models from the present values are shown in Table 4, up to $m = n = 4$. There appears to be an uncertainty of about $2\frac{1}{2}\,\gamma\,\mathrm{yr}^{-1}$ in the determination of the coefficients which masks any systematic changes with time. Only two coefficients show a monotonic change with time, $g_1{}^0$ which is increasing and $g_2{}^0$ which is becoming more negative. The coefficients of Cain, derived mainly from survey data, do not stand out from those from the other analyses, which depend on observatory data.

Table 4

Departures of various secular variation models from the present model in units of $\gamma\,yr^{-1}$

$\dot{g},h$	n	m	(i) Leaton 1955.0	(v) Adam *et al.* 1956.5	(ii) Nagata & Syono 1957.5	(vi) Cain 1960.0	(iv) Leaton *et al.* 1965.0
$\dot{g}$	1	0	−0·3	0·7	3·3	3·7	5·2
$\dot{g}$	1	1	0·0	−4·0	−4·1	−1·2	−1·7
h	1	1	−0·7	0·3	1·6	−4·4	−0·1
$\dot{g}$	2	0	−0·1	−1·6	−1·1	−2·9	−6·2
$\dot{g}$	2	1	−0·1	−0·1	−1·9	−0·2	−1·4
h	2	1	1·9	6·4	2·4	4·1	7·0
$\dot{g}$	2	2	−0·8	4·2	−0·9	−5·4	0·5
h	2	2	−0·4	−2·4	0·5	1·0	−0·6
$\dot{g}$	3	0	−3·3	0·4	−0·7	−3·5	−2·6
$\dot{g}$	3	1	−1·1	0·4	3·4	1·0	2·1
h	3	1	2·4	−5·9	3·3	0·3	−1·7
$\dot{g}$	3	2	−1·3	−2·6	−1·5	−0·3	−4·5
h	3	2	2·0	3·0	1·5	0·5	−0·4
$\dot{g}$	3	3	0·0	−1·7	1·8	−3·6	1·7
h	3	3	−2·4	−0·4	0·9	0·6	−0·9
$\dot{g}$	4	0	2·2	−1·6	−4·0	1·8	1·0
$\dot{g}$	4	1	1·3	2·3	1·0	−0·8	−0·7
h	4	1	−1·0	5·5	1·5	3·7	4·5
$\dot{g}$	4	2	1·2	2·4	2·4	2·6	2·2
h	4	2	−3·3	−2·3	−2·4	−1·4	−2·0
$\dot{g}$	4	3	−0·8	−0·8	−2·8	−1·1	−2·0
h	4	3	−1·8	−2·3	0·2	−1·4	−0·6
$\dot{g}$	4	4	1·6	−1·6	−1·8	−2·6	−2·6
h	4	4	−1·8	1·2	2·1	−2·3	−1·5

5. The centred dipole

Most of the main field can be represented by the first three spherical harmonic coefficients which are equivalent to a magnetic dipole at the centre of the Earth. The moment, M, latitude, ϕ, and longitude, λ, of the northerly end of the axis of the dipole are given by

$$M = R^3\{(g_1{}^0)^2 + (g_1{}^1)^2 + (h_1{}^1)^2\}^{\frac{1}{2}}$$

$$\phi = \tan^{-1} -g_1{}^0\{(g_1{}^1)^2 + (h_1{}^1)^2\}^{-\frac{1}{2}}$$

$$\lambda = \pi + \tan^{-1}\frac{h_1{}^1}{g_1{}^1}.$$

Results from the present analysis and from a number of other analyses with epochs from 1942 to 1965 are given in Table 5 and Fig. 6. The collection of models is not complete, but is thought to include all those where the data reduction and the analysis were carried out by the same authority.

The dipole moment was decreasing at about $11\,\gamma\,\mathrm{yr}^{-1}$ between 1942.5 and 1962.5, with an increasing rate of decrease. This trend is not apparent from the other main field analyses because of the scatter; however, those models which included secular variation coefficients show a similar rate of change. For reasons already given, the analysis of Cain (1966) may not be strictly comparable with the others. In an investigation using analyses back to 1829, Vestine (1962) has shown that the moment has been decreasing at a rather steady $15\,\gamma\,\mathrm{yr}^{-1}$ for the past century and a half. The present analysis suggests that shorter term variations are superimposed on this steady decrease. Changes in the dipole moment have been discussed more fully by Leaton & Malin (1967).

The direction of the dipole axis is remarkably constant in latitude and shows a small but steady westward drift of $0 \cdot 089 \pm 0 \cdot 011\,\mathrm{deg\,yr}^{-1}$. The other analyses tend to confirm this, although, by comparison, the latitude deduced from the coefficients of Vestine (1947) is rather low.

Table 5

Parameters of the centred dipole

| No.	Source	Epoch	MR^{-3} γ	ΔMR^{-3} $\gamma\,\mathrm{yr}^{-1}$	ϕ °N	$\Delta\phi$ deg yr^{-1}	λ °E	$\Delta\lambda$ deg yr^{-1}
		1942.5	31324		78·61		292·23	
				-7 ± 1		0·00		$-0·09$
		1947.5	31291		78·61		291·78	
				-7 ± 1		0.00		$-0·11$
		1952.5	31257		78·63		291·25	
				-13 ± 1		0·00		$-0·07$
		1957.5	31194		78·65		290·88	
				-17 ± 1		0·00		$-0·09$
		1962.5	31111		78·64		290·44	
1	Jones & Melotte (1953)	1942	30970		78·90		291·44	
2	Afanasieva (1947)	1945	30973		78·21		291·21	
3	Vestine *et al.* (1947)	1945	31189	-9	78·56		289·95	
4	Adam *et al.* (1962) (1963)	1955	30986	-11	78·38		291·22	
5	Finch & Leaton (1957)	1955	31200		78·31		291·03	
6	Fougère (1965)	1958.5	31140		78·45		290·48	
7	Nagata & Oguti (1962)	1958.5	30998	-12	78·37		290·44	
8	Cain (1966)	1960	30936	-22	78·58		290·41	
9	Hurwitz *et al.* (1966)	1965	30981		78·60		290·18	
10	Leaton *et al.* (1965)	1965	30987	-16 ± 2	78·56		289·81	
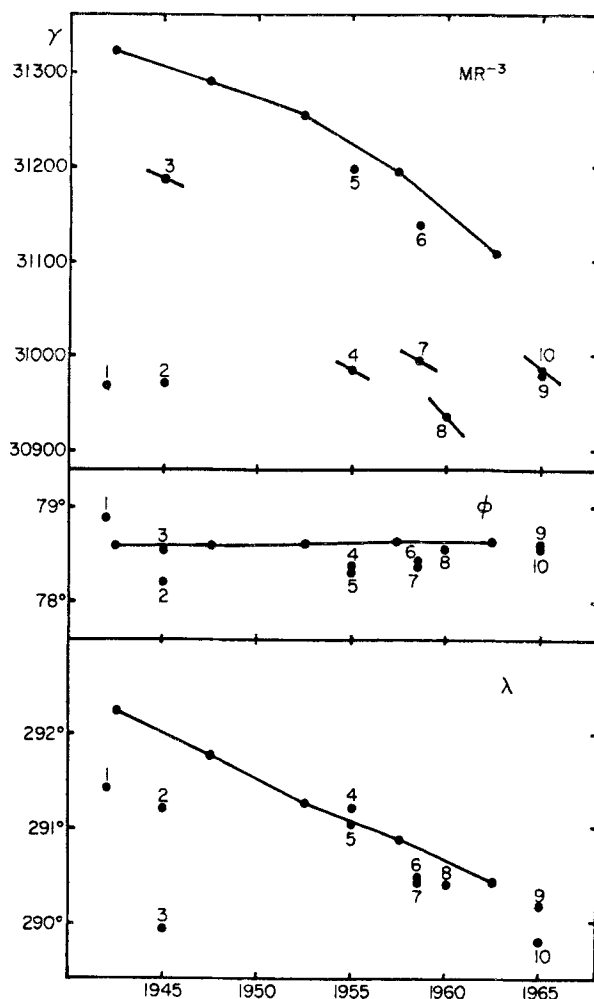
FIG. 6. Parameters of the centred dipole. The numbers correspond with those given in Table 5.

6. The eccentric dipole

The next approximation to the main field is a magnetic dipole displaced from the centre of the Earth to the magnetic centre, C. This dipole has the same moment and direction as the centred dipole. Spherical harmonic coefficients up to $n = 2$ are required to define the eccentric dipole.

The position of the magnetic centre may be expressed in rectangular cartesian co-ordinates as (x_0, y_0, z_0) where x_0 is the north displacement, y_0 is the displacement in the direction of longitude $0°$ and z_0 is the displacement in the direction of longitude $90°$ E, all measured from the centre of the Earth. Equations for x_0, y_0 and z_0 in terms of spherical harmonic coefficients have been derived by Schmidt (1934). The displacement vector may also be expressed in spherical polar co-ordinates $(r_0, \theta_0, \lambda_0)$ where

$$r_0 = (x_0{}^2 + y_0{}^2 + z_0{}^2)^{\frac{1}{2}}$$

$$\theta_0 = \tan^{-1}\{(y_0{}^2 + z_0{}^2)^{\frac{1}{2}}/x_0\}$$

$$\lambda_0 = \tan^{-1}(z_0/y_0).$$

Table 6

Parameters of the magnetic centre

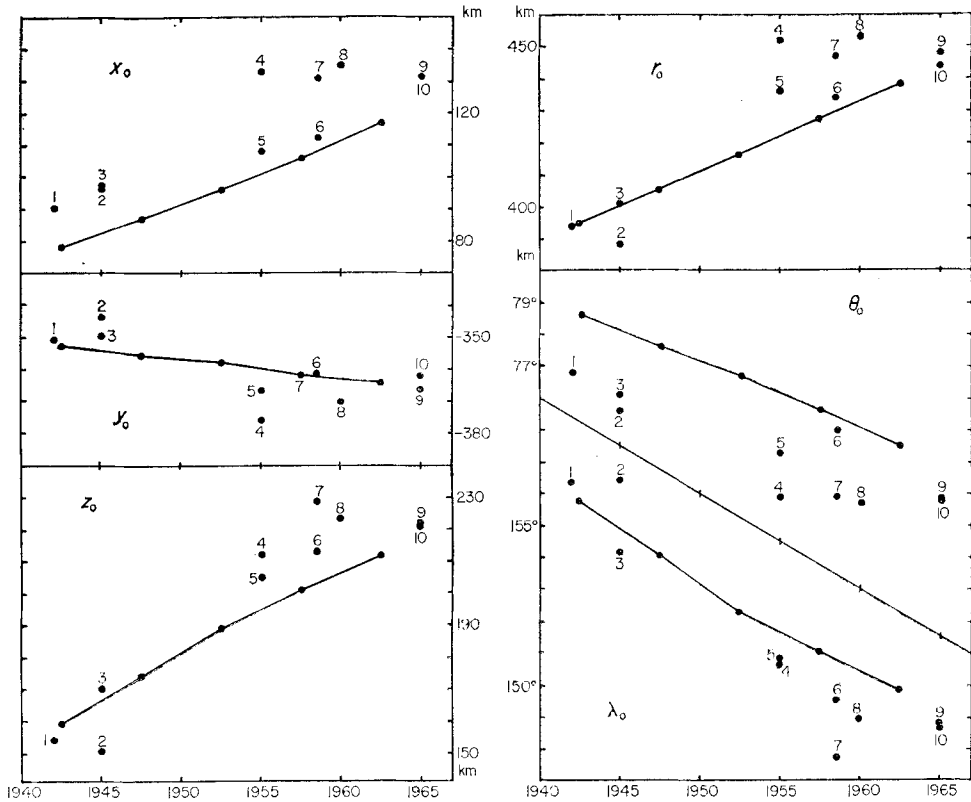| No.	Epoch	x_0 (km)	Δx_0 (km yr^{-1})	y_0 (km)	Δy_0 (km yr^{-1})	z_0 (km)	Δz_0 (km yr^{-1})	r_0 (km)	Δr_0 (km yr^{-1})	θ_0 (deg)	$\Delta\theta_0$ (deg yr^{-1})	λ_0 (deg)	$\Delta\lambda_0$ (deg yr^{-1})
	1942.5	77·9	1·8	−353·1	−0·5	158·8	3·0	394·9	2·1	78·62	−0·20	155·67	−0·34
	1947.5	86·8	1·8	−355·7	−0·5	173·8	3·0	405·3	2·2	77·63	−0·19	153·96	−0·34
	1952.5	96·0	2·0	−358·4	−0·6	188·6	2·4	416·2	2·1	76·66	−0·21	152·25	−0·25
	1957.5	106·2	2·2	−361·6	−0·6	200·6	2·3	426·9	2·2	75·60	−0·23	150·98	−0·23
	1962.5	117·2		−364·5	−0·6	212·1		437·7		74·47		149·81	
1	1942	89·7		−351·3		154·1		394·0		76·84		156·31	
2	1945	96·4		−344·5		150·5		388·1		75·62		156·40	
3	1945	96·6		−350·1		170·1		401·0		76·06		154·09	
4	1955	132·9		−376·4		212·3		452·1		72·90		150·58	
5	1955	117·9		−366·8		204·8		436·3		74·32		150·82	
6	1958.5	112·4		−361·3		212·9		434·2		75·00		149·49	
7	1958.5	131·4		−361·1		228·5		447·1		72·91		147·67	
8	1960	135·0		−370·4		223·6		453·2		72·67		148·88	
9	1965	131·6		−366·3		222·1		448·1		72·92		148·77	
10	1965	131·3		−362·3		220·8		444·1		72·81		148·64	

FIG. 7. Position of the magnetic centre. The numbers correspond with those given
in Table 5.

Results for the present analysis and for the analyses considered in the previous section are given in Table 6 and Fig. 7. The present analysis shows that the eccentric dipole is displaced about 400 km from the centre of the Earth towards a point about $10°$ east of the Marianas Islands. It is moving fairly steadily towards Lanchow, China, at about 3 km yr^{-1}. There is a suggestion that the magnitude of the annual change in z_0 and λ_0 is decreasing, but all of the other parameters show an extremely steady progression with time. The westward drift of the displacement vector is $0 \cdot 29 \pm 0 \cdot 05 \text{ deg yr}^{-1}$, the northward drift is $0 \cdot 21 \pm 0 \cdot 01 \text{ deg yr}^{-1}$ and the radial velocity is $2 \cdot 15 \pm 0 \cdot 05 \text{ km yr}^{-1}$.

Because of the rather large scatter amongst the other analyses, they do little more than add general support to the above conclusions.

Vestine (1953) obtained average values of $0 \cdot 30 \text{ deg yr}^{-1}$ for the westward drift and $0 \cdot 25 \text{ deg yr}^{-1}$ for the northward drift between 1830 and 1950. It appears from his Fig. 4 that the northward drift decreased after about 1900, so there is no conflict between his results and those from the present analysis. Nagata & Syono (1961) deduced values of $0 \cdot 30 \text{ deg yr}^{-1}$, $0 \cdot 20 \text{ deg yr}^{-1}$ and $2 \cdot 2 \text{ km yr}^{-1}$ respectively for the westward, northward and radial velocities of the eccentric dipole between 1955 and 1960. The extremely close agreement with the present results is not altogether surprising, since Nagata & Syono also based their analysis on observatory annual mean values.

<center>S. R. C. Malin</center>

<center>Table 7</center>

<center>*Westward drift*</center>

Latitude (deg)	1942.5 –1947.5 (deg yr^{-1})	1947.5 –1952.5 (deg yr^{-1})	1952.5 –1957.5 (deg yr^{-1})	1957.5 –1962.5 (deg yr^{-1})	1942.5 –1962.5 (deg yr^{-1})	A_m 1952.5 (γ)
			ϕ_1			
80	0·38	0·28	0·14	−0·04	0·20	474
60	0·08	0·06	−0·06	−0·12	−0·01	1294
40	−0·04	0·02	−0·02	0·00	−0·01	2682
20	0·10	0·18	0·08	0·14	0·12	4416
0	0·16	0·20	0·14	0·16	0·16	6094
−20	0·14	0·14	0·10	0·12	0·12	7233
−40	0·08	0·12	0·06	0·08	0·08	7757
−60	0·14	0·16	0·12	0·12	0·14	6570
−80	0·20	0·22	0·18	0·16	0·19	2646
Wt mean					0·11	
			$\dot{\phi}'_1$			
80	0·28	0·28	0·24	0·22	0·26	999
60	0·38	0·34	0·30	0·24	0·32	2166
40	0·44	0·42	0·30	0·28	0·36	2227
20	0·34	0·30	0·22	0·24	0·28	1922
0	0·08	0·14	0·10	0·20	0·13	1349
−20	0·40	0·28	0·24	0·26	0·30	1474
−40	0·22	0·22	0·16	0·16	0·19	3801
−60	0·28	0·28	0·22	0·22	0·25	4372
−80	0·32	0·32	0·32	0·28	0·31	1934
Wt mean					0·26	
			ϕ_2			
80	0·04	0·00	0·00	−0·02	0·00	203
60	0·04	0·02	0·04	0·02	0·03	1365
40	0·08	0·08	0·10	0·10	0·09	2134
20	0·16	0·20	0·22	0·22	0·20	1836
0	0·30	0·40	0·42	0·38	0·38	1159
−20	0·64	0·82	0·76	0·74	0·74	532
−40	1·58	1·70	0·92	0·60	1·20	224
−60	1·10	1·24	0·54	0·48	0·84	212
−80	1·16	1·26	0·54	0·56	0·88	35
Wt mean					0·25	
			ϕ_3			
80	0·02	0·14	0·08	0·04	0·07	10
60	0·02	0·12	0·04	0·00	0·04	134
40	−0·58	−0·20	−0·60	−0·34	−0·43	59
20	0·10	0·20	0·22	0·20	0·18	455
0	0·12	0·06	0·18	0·14	0·12	641
−20	0·18	0·10	0·20	0·18	0·16	638
−40	0·24	0·24	0·20	0·24	0·23	660
−60	0·26	0·28	0·20	0·24	0·24	332
−80	0·26	0·28	0·20	0·22	0·24	19
Wt mean					0·16	

7. Multipoles

An alternative representation may be obtained by considering the geomagnetic field to consist of a series of multipoles at the centre of the Earth. The spherical harmonic coefficients for $n = 1$ represent a dipole (discussed earlier), for $n = 2$ a quadrupole (a closely adjacent pair of dipoles with equal and opposite moments), for $n = 3$ an octupole and so on. Such multipoles give a new outlook on the problem of secular variation. Multipole parameters from the present analysis are presented and discussed elsewhere (Winch & Malin 1968).

8. Westward drift

The westward drift of the geomagnetic field relative to the surface of the Earth was first noted by Halley (1693) who studied the time changes of declination at a number of sites. He concluded that these were caused by a part of the field which was fixed in a solid core rotating more slowly than the surface of the Earth.

More recently westward drift has been the subject of an extensive investigation by Yukatake (1962). For the present analysis the method he described in his Section 2–1 would appear to be the most appropriate. The variation of V around a circle of latitude may be expressed in terms of Fourier coefficients, G_m and H_m

$$V = \sum_{m=1}^{6} (G_m \cos m\lambda + H_m \sin m\lambda) = \sum_{m=1}^{6} A_m \cos m(\lambda - \phi_m)$$

where

$$G_m = \sum_{n=1}^{6} g_n^{\,m} P_n^{\,m}, \qquad H_m = \sum_{n=1}^{6} h_n^{\,m} P_n^{\,m},$$

$$A_m = (G_m^{\,2} + H_m^{\,2})^{\frac{1}{2}}, \qquad \phi_m = \frac{1}{m} \tan^{-1} \frac{H_m}{G_m}.$$

Then the westerly drift, $\dot{\phi}_m$, of the mth harmonic at the chosen latitude is given by the annual decrease in ϕ_m.

Since the centred dipole field appears to drift more slowly than the non-dipole field, it is of interest to consider the two parts separately. The dipole part may be removed by assuming the first three spherical harmonic coefficients to be zero. Only ϕ_1 is affected, and the non-dipole part is denoted ϕ_1'. Values of $\dot{\phi}_m$ and $\dot{\phi}_1'$ are tabulated for $m = 1$ to 3 at 20° intervals of latitude for each of the four five-year intervals between main field analyses and also the mean values for the interval 1942.5 to 1962.5 (Table 7).

Yukatake deduced values of $\dot{\phi}_m$ and $\dot{\phi}_1'$ from the slopes of straight lines drawn through the values of ϕ_m from analyses for nine epochs from 1829 to 1955. All of these analyses were based on grid point values read from charts produced from survey data. Eight different authorities produced the nine analyses, and there was a fairly large scatter about the straight lines. Thus it is remarkable that the mean results from the present analysis which was for a different interval and was based on observatory data should agree so well with the results of Yukatake (Fig. 8). This agreement gives added confidence both to Yukatake's analysis and to the present analysis, as well as confirming that many of the smaller scale features which might have been thought to be spurious, are in fact, real.

The westward drift also shows a number of shorter-lived features (Fig. 9) to which credence is given by the steady change from epoch to epoch. The most notable of these is the peak in $\dot{\phi}_2$ at 40° S which passed through a maximum near 1950. The latitudinal variations in $\dot{\phi}_1'$ are smoothing out and the northerly part of the $\dot{\phi}_1$ curve changed to a small easterly drift near 1958.
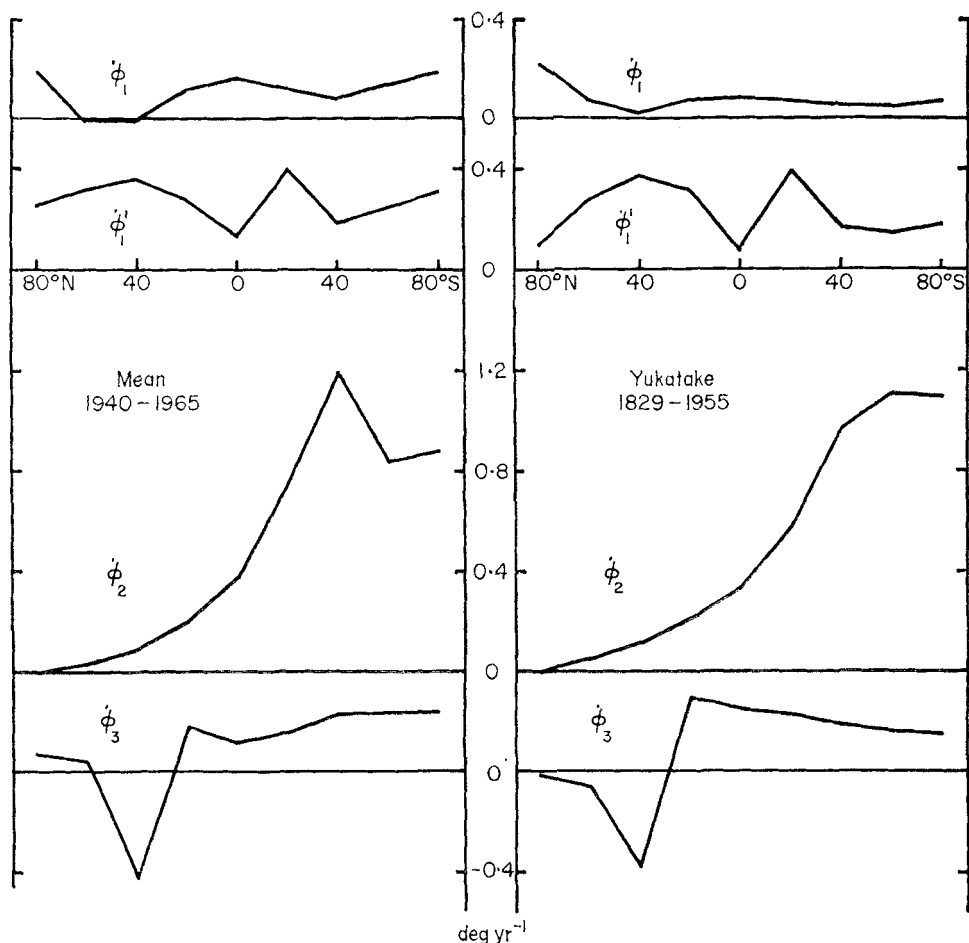
FIG. 8. Westward drift of Fourier coefficients.

In view of the variation of westward drift with latitude and between different values of m, it is clear that a non-dipole field rotating steadily with respect to the Earth's surface is too simple a model. However, an appreciable part of the secular variation field can be represented in this way and it is of interest to calculate a mean value for westward drift. Most of the extreme values of $\dot{\phi}_m$ occur when A_m is small, therefore, in calculating the mean, the values of $\dot{\phi}_m$ were weighted according to A_m. These weighted means up to $m = 3$ are included in Table 7. The mean value for westward drift for the non-dipole field up to $m = 6$ is $0°\cdot25$ per year.

An alternative approach is to determine the westward drift, d_n, of each multipole from the relation

$$d_n = 57\cdot3 \frac{\sum\limits_m (\dot{g}_n{}^m h_n{}^m - g_n{}^m \dot{h}_n{}^m)}{\sum\limits_m [(g_n{}^m)^2 + (h_n{}^m)^2]} \ \text{deg yr}^{-1}.$$

By choosing appropriate weights for d_n, Richmond (1966) has used this method to determine the mean westward drift from the geomagnetic potential, $D(V)$, and for the radial component of the field, $D(Z)$, at the surface of the Earth and at the core–mantle boundary ($r = 3471$ km). The values obtained by Richmond using the spherical harmonic coefficients of Hendricks & Cain (1966), and values from the
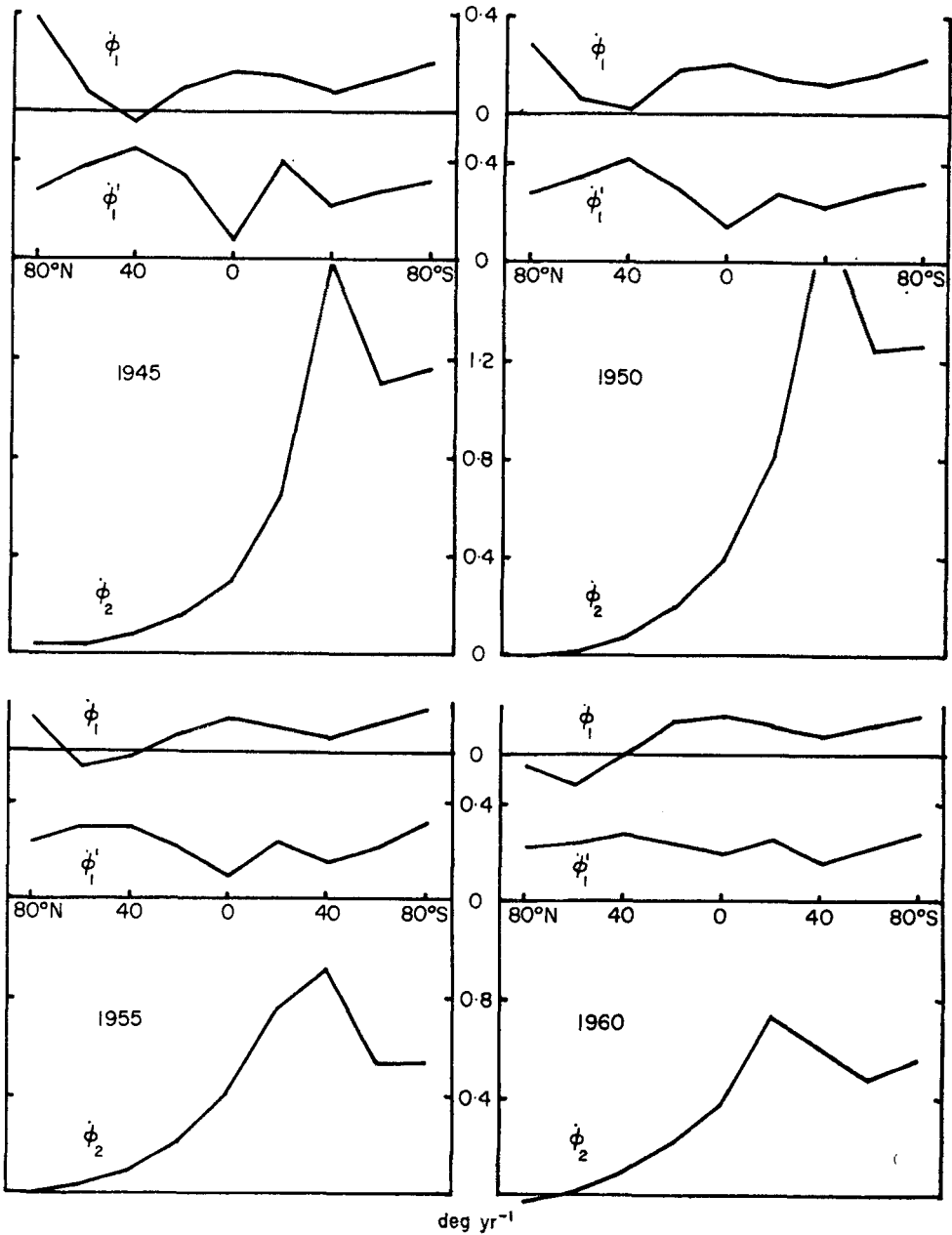
Fig. 9. Westward drift of Fourier coefficients—four epochs.

present analysis using the weights of Richmond, are shown in Table 8. The Hendricks & Cain secular variation coefficients are those required to make successive surveys compatible and do not depend very strongly on observatory data. This is probably the reason for the differences between the two sets of results.

Since d_2 is by far the largest of the multipole drifts it is clear that the value of D will depend very greatly on the weight given to d_2. At the core–mantle boundary the higher multipoles are given much greater weight than d_2, so the deduced values of D are much lower than at the surface.

Table 8

Westward drift by Richmond's method

		Richmond (deg yr^{-1})	Malin (deg yr^{-1})
	d_1	0·0395	0·0980
	d_2	0·2205	0·2828
	d_3	0·1116	0·0985
	d_4	0·1843	0·1234
	d_5	−0·0055	0·0504
	d_6	0·0975	0·1548
$D(V)$ Surface,	$n = 1$ to 6	0·0930	0·1344
$D(V)$ Surface,	$n = 2$ to 6	0·1779	0·2063
$D(Z)$ Surface,	$n = 1$ to 6	0·1204	0·1465
$D(Z)$ Surface,	$n = 2$ to 6	0·1590	0·1739
$D(V)$ Core	$n = 1$ to 6	0·1123	0·1327
$D(V)$ Core	$n = 2$ to 6	0·1200	0·1373
$D(Z)$ Core	$n = 1$ to 6	0·1008	0·1291
$D(Z)$ Core	$n = 2$ to 6	0·1017	0·1297
$D(Z)$ Core	$n = 1$ to 5	0·1040	0·1050
$D(Z)$ Core	$n = 1$ to 4	0·1552	0·1305

Other methods of determining westward drift involve the use of magnetic charts. Bullard *et al.* (1950) deduced a value of $0·18 \pm 0·015$ deg yr^{-1} for the westward drift of the non-dipole field between 1907 and 1945 from a comparison of magnetic charts for these epochs. Leaton (1962) compared secular change and main field charts for the epoch 1955. Although the charts used in these investigations were smoothed, it is likely that they contained some local anomalies with wavelengths too small to be represented by a sixth order analysis. Short wavelength anomalies originate near to the surface, and would not be expected to share in the westward drift. Thus values deduced by these methods will probably be less than the rate of drift of the core sources since a proportion of non-drifting sources are included. For this reason values obtained by these methods are likely to be lower than values obtained from sixth order spherical harmonic coefficients.

9. Surface motions of the Earth's core

Although much of the observed secular variation can be accounted for by a westward drift of the core relative to the crust, it is clear that a more complex motion is required to explain the variations of drift in various parts of the world. Kahle *et al.* (1967a) have derived a method for deducing the motion of the surface of the core from the vertical components of the main field and secular variation, making the assumptions that, at the surface of the core, transverse movements of the magnetic field are associated with identical movements of the core, that the core material is incompressible and that equation (1) is valid throughout the region between the crust and the core. They separate the surface flow into an irrotational part derivable from a potential ψ given in surface harmonics by

$$\psi = a \sum_n \sum_m (\alpha_n^m \cos m\lambda + \beta_n^m \sin m\lambda) \, P_n^m(\cos \theta)$$

where a is the radius of the core, and a rotational part for which the stream function χ is given by

$$\chi = \sum_n \sum_m (A_n^m \cos m\lambda + B_n^m \sin m\lambda) \, P_n^m(\cos \theta).$$

The $A_n{}^0$ terms describe the rotation about the geographical axis, which is equivalent to westward drift. The surface velocity $\mathbf{v}$ may be deduced from these functions using the relation

$$\mathbf{v} = -\nabla_T \psi + \mathbf{a} \times \nabla \chi$$

where the subscript T denotes the tangential (horizontal) component of the gradient, and $\mathbf{a}$ is equal to a times the unit vector in the radial direction.

Kahle *et al.* (1967a) applied this method to the 1955 main field model of Vestine *et al.* (1963) and the secular variation for the interval 1912 to 1955 (Vestine *et al.* 1947; Nagata & Syono 1961). The first six orders of the main field and secular variation were used, extrapolated down to a hypothetical core of radius 4000 km. This radius was chosen to avoid excessive amplification of the higher order coefficients. Spherical harmonic coefficients of the potential and rotational parts of the flow were evaluated up to $m = n = 4$.

Kahle *et al.* (1967b) have also applied the method to sets of coefficients for the main field and secular variation from various sources for epoch 1885, 1912, 1933 and 1960. Main field coefficients up to $m = n = 6$ and secular variation coefficients up to $m = n = 4$ were used. The core radius was assumed to be 3471 km. Although there is considerable variation between epochs in the flow pattern obtained from these analyses, they all show a strong positive focus in ψ just south of Africa. Since the potential part of the fluid motion is perpendicular to the isolines of ψ, a positive focus indicates a source, which may be interpreted as a region of upflow. There is also a suggestion of a weaker downflow in the vicinity of the North Pacific. In all cases the westward drift is large in southern latitudes and small, or even negative, in northern latitudes. In the case of the rotational part, flow is parallel to the stream lines, clockwise for positive values. The rotational flow, after removal of the westward drift, shows four persistent rotating cells, two clockwise and two anticlockwise. The magnitude of the rotational part of the motion is greater than the magnitude of the potential part.

Table 9

Spherical harmonic coefficients of velocity field in km yr^{-1}

| α, β | n | m | \multicolumn{4}{c}{Potential field, ψ} | A, B | \multicolumn{4}{c}{Rotational field, χ} |
|---|---|---|---|---|---|---|---|---|---|---|---|
| | | | 1945 | 1950 | 1955 | 1960 | | 1945 | 1950 | 1955 | 1960 |
| α | 1 | 0 | −0·834 | −1·591 | −1·573 | −1·426 | A | 6·186 | 8·015 | 3·843 | 5·269 |
| α | 1 | 1 | −1·961 | −1·088 | −0·629 | −1·404 | A | −1·982 | 0·171 | −0·399 | −0·301 |
| β | 1 | 1 | −0·865 | −0·860 | −0·852 | −1·019 | B | 2·487 | 2·766 | 1·477 | 1·183 |
| α | 2 | 0 | 0·146 | 0·328 | 0·093 | 0·036 | A | −2·752 | −3·310 | −2·832 | −3·251 |
| α | 2 | 1 | −0·592 | −0·802 | −0·469 | −0·533 | A | 3·362 | 2·511 | 2·404 | 2·707 |
| β | 2 | 1 | −0·999 | −1·332 | −1·092 | −1·088 | B | 1·149 | 0·208 | 0·170 | 0·614 |
| α | 2 | 2 | −0·726 | −1·402 | −0·830 | −1·142 | A | 1·710 | 2·031 | 2·288 | 1·832 |
| β | 2 | 2 | 0·071 | 0·368 | 0·049 | 0·178 | B | −0·129 | −0·703 | −0·287 | −0·168 |
| α | 3 | 0 | −0·038 | 0·013 | 0·092 | −0·049 | A | 0·311 | 0·331 | 0·892 | 0·392 |
| α | 3 | 1 | 0·389 | −0·129 | −0·160 | −0·201 | A | −1·339 | −1·831 | −2·560 | −2·485 |
| β | 3 | 1 | 0·047 | −0·098 | 0·075 | 0·287 | B | −2·407 | −2·161 | −1·501 | −1·447 |
| α | 3 | 2 | −0·127 | −0·074 | −0·272 | −0·170 | A | 0·620 | 0·724 | 1·047 | 1·150 |
| β | 3 | 2 | 0·402 | 0·428 | 0·566 | 0·347 | B | 0·734 | 1·199 | 0·263 | −0·072 |
| α | 3 | 3 | 0·704 | 0·513 | 0·360 | 0·073 | A | 0·361 | 0·137 | 1·131 | 0·667 |
| β | 3 | 3 | −0·269 | −0·596 | −0·887 | −0·985 | B | −0·519 | −0·861 | −0·336 | −0·299 |
| α | 4 | 0 | 0·574 | 0·375 | 0·236 | 0·218 | A | 0·340 | −0·179 | 0·497 | 0·073 |
| α | 4 | 1 | 0·408 | 0·311 | 0·096 | −0·009 | A | −0·354 | −0·472 | −0·088 | −0·140 |
| β | 4 | 1 | 0·229 | 0·301 | 0·520 | 0·247 | B | −0·061 | 0·977 | 0·707 | 0·801 |
| α | 4 | 2 | 0·417 | 0·291 | 0·285 | 0·248 | A | 0·760 | 0·356 | 0·643 | 1·039 |
| β | 4 | 2 | 0·043 | 0·139 | 0·452 | 0·237 | B | −0·528 | −0·937 | −0·756 | −1·117 |
| α | 4 | 3 | 0·291 | 0·181 | 0·085 | −0·113 | A | −0·286 | 0·169 | −0·654 | −0·489 |
| β | 4 | 3 | −0·334 | −0·151 | −0·172 | −0·274 | B | −0·014 | −0·456 | −0·533 | −0·637 |
| α | 4 | 4 | 0·259 | 0·116 | 0·005 | −0·098 | A | 0·732 | 0·682 | 0·263 | 0·181 |
| β | 4 | 4 | −0·099 | −0·059 | 0·079 | 0·030 | B | −0·085 | −0·697 | −0·915 | −0·526 |
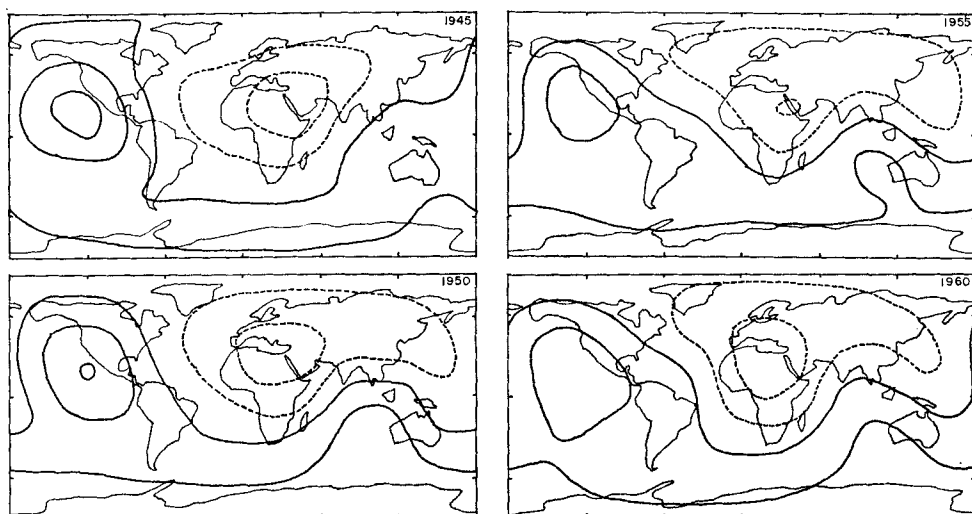
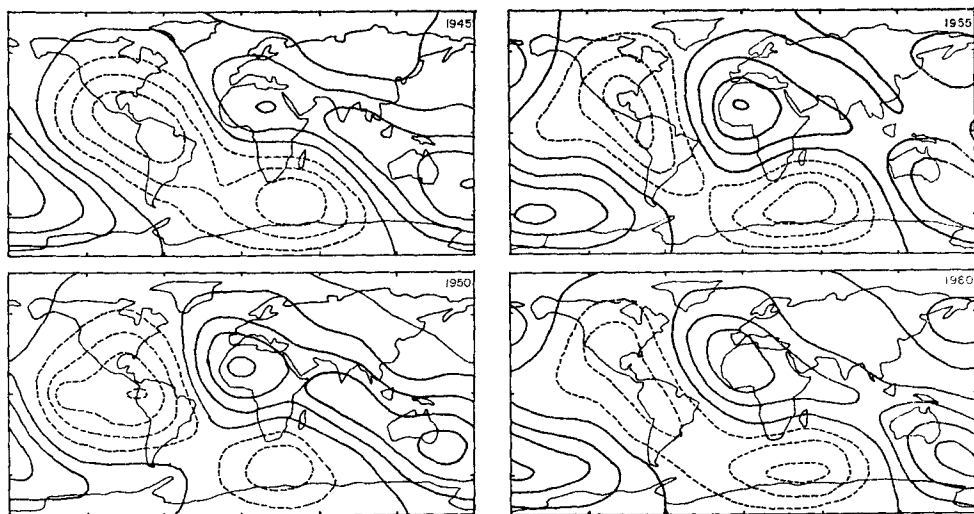FIG. 10. Potential flow at the surface of the core—four epochs. (Contour interval = 5000 km^2 yr^{-1})

FIG. 11. Rotational flow at the surface of the core—four epochs. (Contour interval = 5000 km^2 yr^{-1})

The data from the present analysis have been subjected to a similar analysis for fluid motions. In this case, the core radius was taken to be 3471 km and all six orders of secular variation (Table 3) were used. The main field coefficients for 1952.5 (Table 2) were used for all four epochs. Spherical harmonic coefficients up to $m = n = 4$ for the fluid motions are presented in Table 9. The changes from epoch to epoch are much more erratic for the fluid motion coefficients than for the original secular variation coefficients. This is probably because of the amplification of the higher order secular variation coefficients and their associated errors, because of extrapolation down to the core surface. The relatively poorly determined sixth order coefficients are multiplied by a factor of $(R/a)^8 = 129$. However, it is interesting to note that it is the *lower* order coefficients for the fluid motions which are the most erratic.

Fig. 10 shows contours of equal ψ at the surface of the core synthesised from these coefficients. The four epochs all show similar patterns, with two regions of upflow,

one in Antarctica and one in the Eastern Pacific, and one region of downflow centred on the Mediterranian. However they bear very little relation to the comparable figures of Kahle *et al.* (1967a, 1967b).

The stream lines of the rotating part *minus* the westward drift are shown in Fig. 11. The four epochs are self consistent, and have some features in common with the comparable figures of Kahle *et al.* (1967a, 1967b). Both authors have a four cell pattern, two clockwise and two anticlockwise, with amplitudes greater than for the potential flow. The two clockwise cells are over Africa and the South Pacific, and one of the anticlockwise cells is south of Africa. The present results place the second
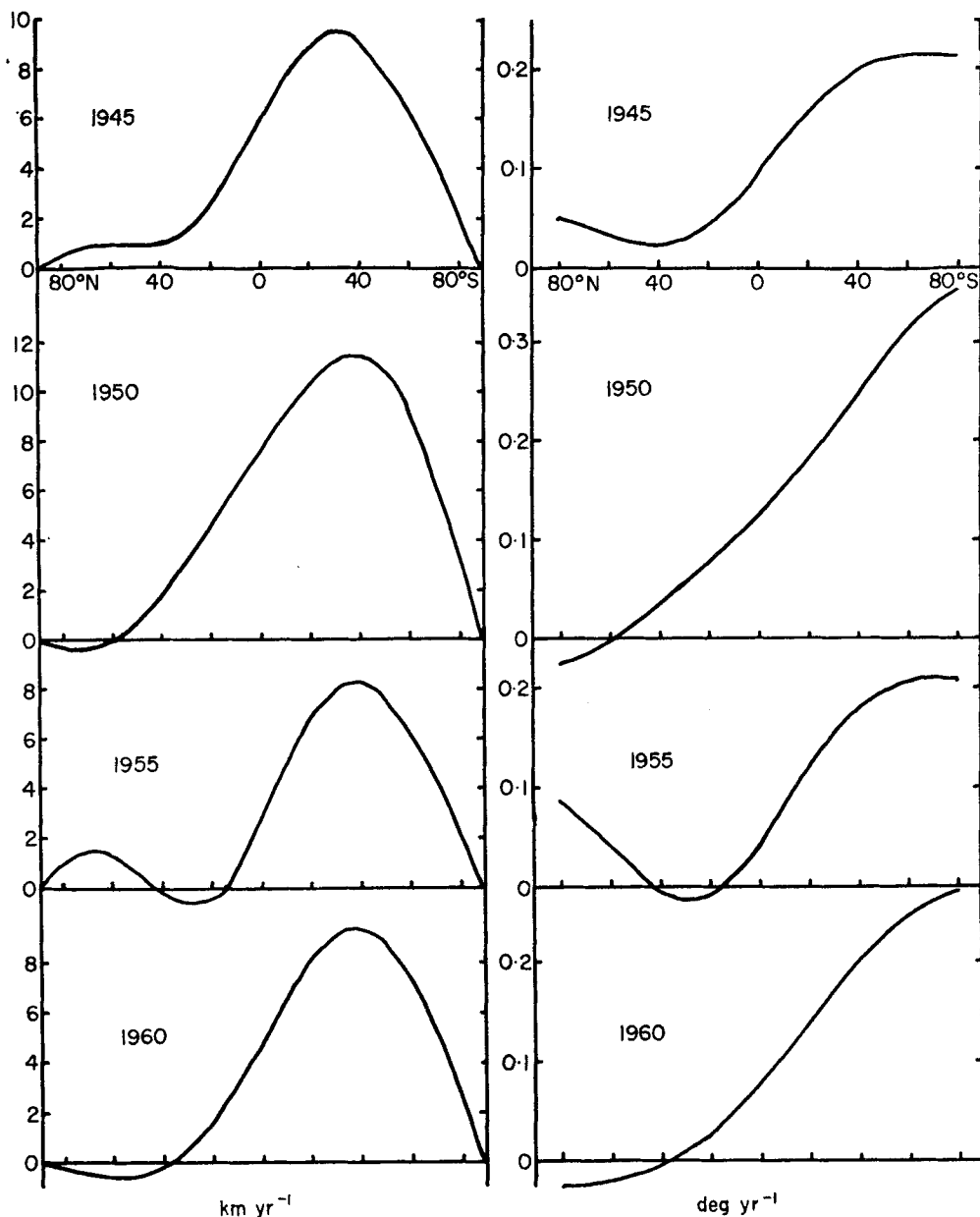
FIG. 12. Westward drift by Kahle's method.

anticlockwise cell over Central America whereas Kahle *et al.* place it over the central Pacific.

Westward drift (Fig. 12) is fairly well-behaved, with small or eastward drift in northern latitudes and a large westward drift in the south. The mean value for the westward drift is $0 \cdot 96$ deg yr^{-1}; however, this method is not particularly reliable for the determination of westward drift, since motion parallel to the isolines of Z, which tend to run east–west, would not affect secular variation and would not be detected.

10. Secular acceleration

From a study of the spherical harmonic coefficients of secular variation in Table 3 and from the behaviour of the eccentric dipole it is clear that the secular variation field is changing fairly steadily with time. For this reason it is possible to represent most of the changes with time as a steady secular acceleration. It should be pointed out, however, that the secular change pattern has been suspected of varying erratically in the past, and the use of the secular acceleration for extrapolation outside the interval 1940–65 should be treated with caution.

The four determinations of secular change are considered to be independent. This assumption would be strictly true only if the data in Table 1 were completely free from error. Spherical harmonic coefficients for secular acceleration may then be derived from the relations

$$\ddot{g}_n^m = 0 \cdot 02 \left(-3\dot{g}_n^m{}_{1945} - \dot{g}_n^m{}_{1950} + \dot{g}_n^m{}_{1955} + 3\dot{g}_{n\,1960}^m \right) \gamma \, \text{yr}^{-2},$$

$$\ddot{h}_n^m = 0 \cdot 02 \left(-3\dot{h}_n^m{}_{1945} - \dot{h}_n^m{}_{1950} + \dot{h}_n^m{}_{1955} + 3\dot{h}_n^m{}_{1960} \right) \gamma \, \text{yr}^{-2}.$$

This is equivalent to fitting a straight line through the four secular variation coefficients by the method of least squares. For reasons discussed earlier, secular acceleration coefficients derived in this way are the same as would be derived from an analysis of secular acceleration for each observatory. The standard deviations are deduced from the secular variation residuals in a similar way.

Table 10

Spherical harmonic coefficients of the secular acceleration field

| g, h	n	m	1942.5–1962.5 (γ yr^{-2})	g, h	n	m	1942.5–1962.5 (γ yr^{-2})	g, h	n	m	1942.5–1962.5 (γ yr^{-2})
g	1	0	$0 \cdot 70 \pm 0 \cdot 11$	g	4	1	$-0 \cdot 15 \pm 0 \cdot 07$	h	5	4	$0 \cdot 09 \pm 0 \cdot 07$
g	1	1	$-0 \cdot 02 \quad 0 \cdot 13$	h	4	1	$0 \cdot 06 \quad 0 \cdot 09$	g	5	5	$-0 \cdot 03 \quad 0 \cdot 09$
h	1	1	$-0 \cdot 15 \quad 0 \cdot 13$	g	4	2	$-0 \cdot 13 \quad 0 \cdot 07$	h	5	5	$0 \cdot 11 \quad 0 \cdot 09$
g	2	0	$-0 \cdot 20 \quad 0 \cdot 11$	h	4	2	$0 \cdot 04 \quad 0 \cdot 09$	g	6	0	$0 \cdot 06 \quad 0 \cdot 06$
g	2	1	$-0 \cdot 06 \quad 0 \cdot 10$	g	4	3	$-0 \cdot 05 \quad 0 \cdot 07$	g	6	1	$0 \cdot 05 \quad 0 \cdot 05$
h	2	1	$0 \cdot 50 \quad 0 \cdot 11$	h	4	3	$-0 \cdot 07 \quad 0 \cdot 07$	h	6	1	$-0 \cdot 06 \quad 0 \cdot 05$
g	2	2	$0 \cdot 25 \quad 0 \cdot 12$	g	4	4	$-0 \cdot 28 \quad 0 \cdot 09$	g	6	2	$0 \cdot 09 \quad 0 \cdot 05$
h	2	2	$-0 \cdot 06 \quad 0 \cdot 13$	h	4	4	$0 \cdot 25 \quad 0 \cdot 09$	h	6	2	$0 \cdot 01 \quad 0 \cdot 05$
g	3	0	$-0 \cdot 40 \quad 0 \cdot 09$	g	5	0	$-0 \cdot 08 \quad 0 \cdot 08$	g	6	3	$0 \cdot 17 \quad 0 \cdot 06$
g	3	1	$0 \cdot 04 \quad 0 \cdot 08$	g	5	1	$-0 \cdot 16 \quad 0 \cdot 07$	h	6	3	$-0 \cdot 05 \quad 0 \cdot 05$
h	3	1	$0 \cdot 30 \quad 0 \cdot 11$	h	5	1	$-0 \cdot 05 \quad 0 \cdot 07$	g	6	4	$-0 \cdot 04 \quad 0 \cdot 06$
g	3	2	$-0 \cdot 26 \quad 0 \cdot 08$	g	5	2	$0 \cdot 05 \quad 0 \cdot 06$	h	6	4	$-0 \cdot 08 \quad 0 \cdot 06$
h	3	2	$-0 \cdot 19 \quad 0 \cdot 09$	h	5	2	$0 \cdot 16 \quad 0 \cdot 07$	g	6	5	$0 \cdot 07 \quad 0 \cdot 05$
g	3	3	$0 \cdot 05 \quad 0 \cdot 10$	g	5	3	$-0 \cdot 06 \quad 0 \cdot 08$	h	6	5	$-0 \cdot 01 \quad 0 \cdot 06$
h	3	3	$-0 \cdot 09 \quad 0 \cdot 10$	h	5	3	$0 \cdot 08 \quad 0 \cdot 07$	g	6	6	$-0 \cdot 08 \quad 0 \cdot 08$
g	4	0	$-0 \cdot 15 \quad 0 \cdot 09$	g	5	4	$0 \cdot 03 \quad 0 \cdot 07$	h	6	6	$-0 \cdot 05 \quad 0 \cdot 08$
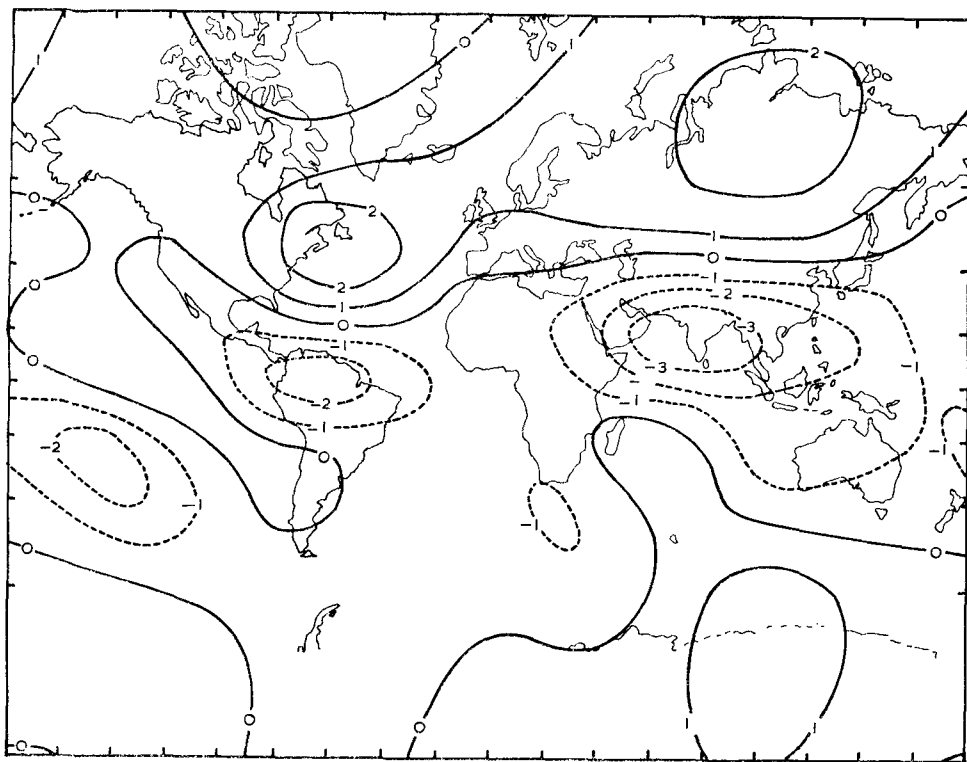
FIG. 13. Secular acceleration in X in units of $\gamma\,\mathrm{yr}^{-2}$.

Spherical harmonic coefficients of secular acceleration and their standard deviations are shown in Table 10. Charts of $\ddot{X}$, $\ddot{Y}$ and $\ddot{Z}$ deduced from these coefficients are shown in Figs 13–15. The charts are on Mercator's projection and extend from 80° N to 80° S. Contours are drawn at intervals of one gamma per year per year with positive and zero values shown by solid lines and negative values shown by broken lines.

The $\ddot{X}$ chart suggests that the two Atlantic secular change foci in X are deepening and moving to the west, and the region of positive change in south Asia and the Indian Ocean is rapidly decreasing. The Antarctic focus is fairly steady, but a negative focus may build up in the South Pacific.

The $\ddot{Y}$ chart suggests that the South American focus of secular change in Y is getting deeper, but becoming more localized and that the South Indian Ocean focus is moving further south. The Greenwich meridian focus remains at the same depth, but is spreading towards the east, while the value at the South Pole remains steady.

As in the case of secular change, $\ddot{Z}$ shows deeper foci and steeper gradients than the other elements. The secular change focus in the Atlantic is deepening and moving north-west, while the other negative focus in the Indian Ocean is losing its northerly lobe, decreasing in amplitude and moving south-west. There is little activity over the Antarctic, but a slight suggestion that the Antarctic focus is dividing into two, as is shown on the British and American world charts of secular change for 1965. The small European focus is decreasing and moving north-west.
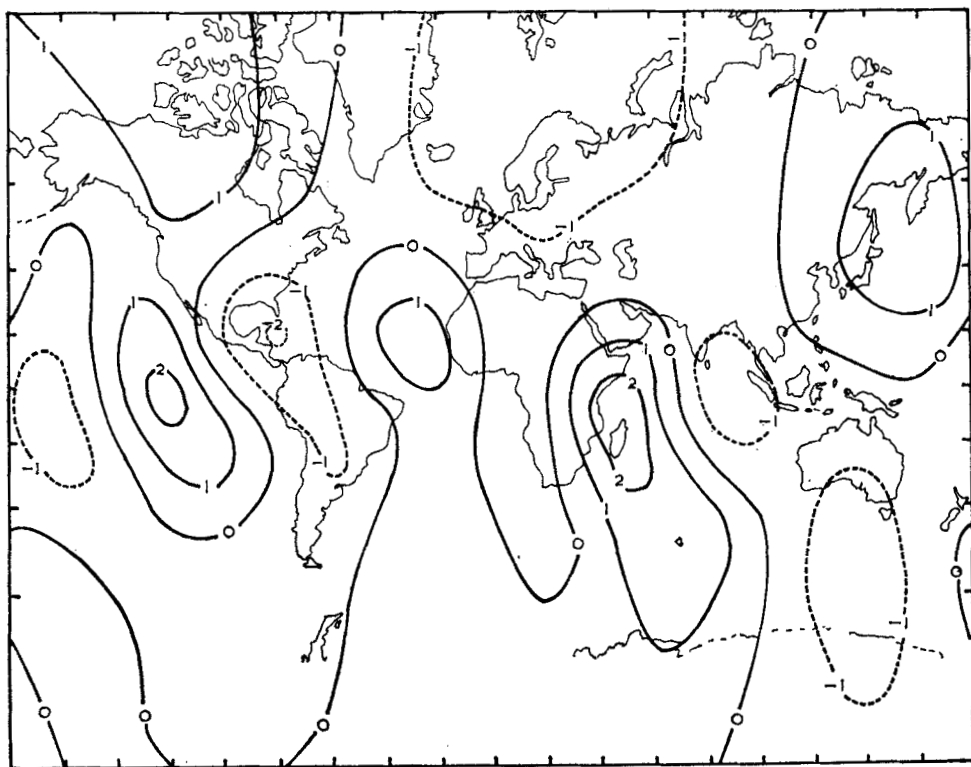
FIG. 14. Secular acceleration in Y in units of $\gamma \, \mathrm{yr}^{-2}$.
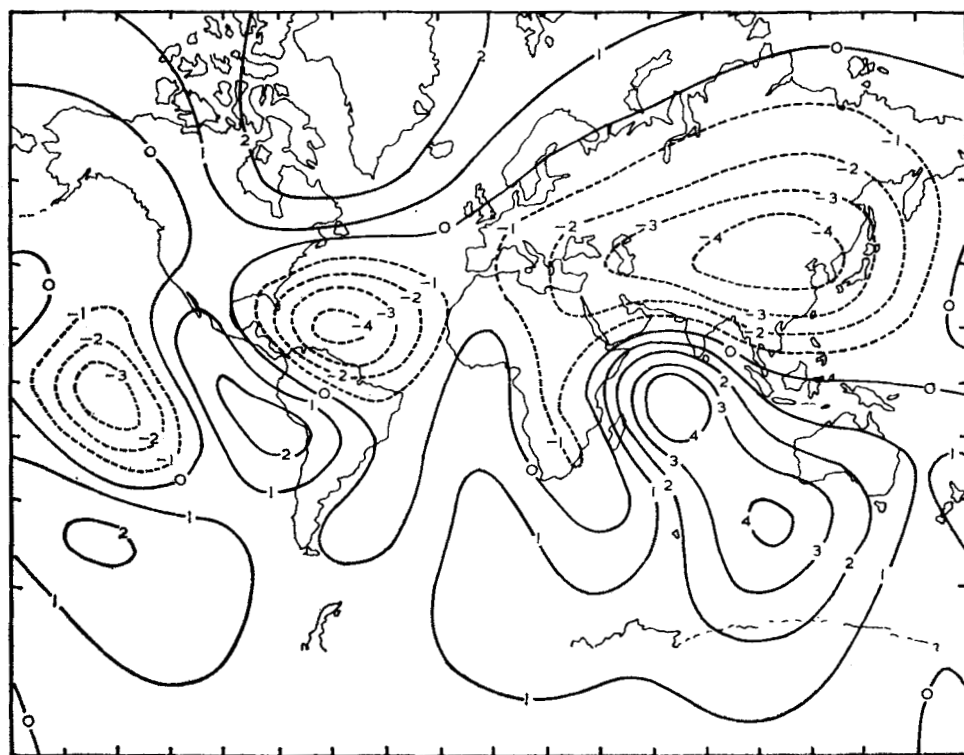
FIG. 15. Secular acceleration in Z in units of $\gamma \, \mathrm{yr}^{-2}$.

Acknowledgments

References

Adam, N. V., Benkova, N. P., Orlov, V. P., Osipov, N. K. & Tiurmina, L. O., 1962. *Geomag. Aeron., U.S.S.R.*, **2**, 949.

Adam, N. V., Benkova, N. P., Orlov, V. P., Osipov, N. K. & Tiurmina, L. O., 1963. *Geomag. Aeron., U.S.S.R.*, **3**, 336.

Afanasieva, V. I., 1946. *Terr. Magn. atmos. Elect.*, **51**, 19.

Bullard, E. C., Freedman, Cynthia, Gellman, H. & Nixon, Jo, 1950. *Phil. Trans. R. Soc.*, **A243**, 67.

Cain, J. C., 1966. *Radiation Trapped in the Earth's Magnetic Field*, ed. by Billy M. McCormac, p. 7, Reidel, Dordrecht.

Cain, J. C., 1967. Quoted in: *Geophys. J. R. astr. Soc.*, **12**, 521.

Finch, H. F. & Leaton, B. R., 1957. *Mon. Not. R. astr. Soc., geophys. Suppl.*, **7**, 314.

Fougère, P. F., 1965. *J. geophys. Res.*, **70**, 2171.

Halley, E., 1693. *Phil. Trans. R. Soc.*, **17**, 563.

Hendricks, S. J. & Cain, J. C., 1966. *J. geophys. Res.*, **71**, 346.

Hurwitz, L., Knapp, D. G., Nelson, J. H. & Watson, D. E., 1966. *J. geophys. Res.*, **71**, 2373.

Jones, H. S. & Melotte, P. J., 1953. *Mon. Not. R. astr. Soc., geophys. Suppl.*, **6**, 409.

Kahle, Anne B., Vestine, E. H. & Ball, R. H., 1967a. *J. geophys. Res.*, **72**, 1095.

Kahle, Anne B., Ball, R. H. & Vestine, E. H., 1967b. *J. geophys. Res.*, **72**, 4917.

Leaton, B. R., 1962. *R. Obs. Bull.* No. 57.

Leaton, B. R., Malin, S. R. C. & Evans, Margaret J., 1965. *J. geomagn. geoelect., Kyoto*, **17**, 187.

Leaton, B. R. & Malin, S. R. C., 1967. *Nature, Lond.*, **213**, 1110.

Malin, S. R. C. & Pocock, Susan B., 1969. *Pure appl. Geophys.*, **73**, 111.

Nagata, T. & Syono, Y., 1961. *J. geomagn. geoelect., Kyoto*, **12**, 84.

Nagata, T. & Oguti, T., 1962. *J. geomagn. geoelect., Kyoto*, **14**, 125.

Orlov, V. P., 1965. *J. geomagn. geolect., Kyoto*, **17**, 277.

Richmond, A. D., 1966. RAND Corporation, Memorandum RM-5191-NASA.

Schmidt, A., 1934. *Gerlands Beiträge Geophysik*, **56**, 346.

Vestine, E. H., Lange, Isabelle, Laporte, Lucile & Scott, W. E., 1947. Carnegie Institution of Washington, Publication 580.

Vestine, E. H., 1953. *J. geophys Res.*, **58**, 127.

Vestine, E. H., 1962. *Proceedings of the Benedum Earth Magnetism Symposium*, p. 57, Pittsburgh.

Vestine, E. H., Sibley, W. L., Kern, J. W. & Carlstedt, J. L., 1963. *J. geomagn. geoelect., Kyoto*, **15**, 47.

Winch, D. E. & Malin, S. R. C., 1968. *Pure appl. Geophys.*, **70**, 177.

Yukatake, T., 1962. *Bull. Earthq. Res. Inst. Tokyo Univ.*, **40**, 1.

Yukatake, T., 1965. *J. geomagn. geoelect., Kyoto*, **17**, 287.